

UC Davis

UC Davis Previously Published Works

Title

Populations of in silico myocytes and tissues reveal synergy of multiatrial-predominant K⁺-current block in atrial fibrillation

Permalink

<https://escholarship.org/uc/item/2vw0w1dx>

Journal

British Journal of Pharmacology, 177(19)

ISSN

0007-1188

Authors

Ni, Haibo

Iseppe, Alex Fogli

Giles, Wayne R

et al.

Publication Date

2020-10-01



DOI

10.1111/bph.15198

Peer reviewed

RESEARCH PAPER

Populations of in silico myocytes and tissues reveal synergy of multiatrial-predominant K^+ -current block in atrial fibrillation

Haibo Ni¹  | Alex Fogli Iseppe¹ | Wayne R. Giles² | Sanjiv M. Narayan³ | Henggui Zhang⁴ | Andrew G. Edwards¹ | Stefano Morotti¹ | Eleonora Grandi¹ 

¹Department of Pharmacology, University of California, Davis, CA, USA

²Faculties of Kinesiology and Medicine, University of Calgary, Calgary, Alberta, Canada

³Division of Cardiology, Cardiovascular Institute, Stanford University, Stanford, CA, USA

⁴Biological Physics Group, School of Physics and Astronomy, The University of Manchester, Manchester, UK

Correspondence

Eleonora Grandi, Department of Pharmacology, University of California, Davis, CA, USA.

Email: ele.grandi@gmail.com

Funding information

National Heart, Lung, and Blood Institute, Grant/Award Numbers: K99HL138160, P01HL141084, R01HL131517, R01HL141214; UC Davis School of Medicine Dean's Fellow Award; Health and Environmental Sciences Institute, Grant/Award Number: U01FD006676; National Institutes of Health (NIH) Stimulating Peripheral Activity to Relieve Conditions, Grant/Award Number: OT2OD026580; American Heart Association Grant and Postdoctoral Fellowship, Grant/Award Numbers: 15SDG24910015, 20POST35120462

Background and Purpose: Pharmacotherapy of atrial fibrillation (AF), the most common cardiac arrhythmia, remains unsatisfactory due to low efficacy and safety concerns. New therapeutic strategies target atrial-predominant ion-channels and involve multichannel block (poly)therapy. As AF is characterized by rapid and irregular atrial activations, compounds displaying potent antiarrhythmic effects at fast and minimal effects at slow rates are desirable. We present a novel systems pharmacology framework to quantitatively evaluate synergistic anti-AF effects of combined block of multiple atrial-predominant K^+ currents (ultra-rapid delayed rectifier K^+ current, I_{Kur} , small conductance Ca^{2+} -activated K^+ current, I_{KCa} , $K_{2P3.1}$ 2-pore-domain K^+ current, I_{K2P}) in AF.

Experimental Approach: We constructed experimentally calibrated populations of virtual atrial myocyte models in normal sinus rhythm and AF-remodelled conditions using two distinct, well-established atrial models. Sensitivity analyses on our atrial populations was used to investigate the rate dependence of action potential duration (APD) changes due to blocking I_{Kur} , I_{K2P} or I_{KCa} and interactions caused by blocking of these currents in modulating APD. Block was simulated in both single myocytes and one-dimensional tissue strands to confirm insights from the sensitivity analyses and examine anti-arrhythmic effects of multi-atrial-predominant K^+ current block in single cells and coupled tissue.

Key Results: In both virtual atrial myocytes and tissues, multiple atrial-predominant K^+ -current block promoted favourable positive rate-dependent APD prolongation and displayed positive rate-dependent synergy, that is, increasing synergistic antiarrhythmic effects at fast pacing versus slow rates.

Conclusion and Implications: Simultaneous block of multiple atrial-predominant K^+ currents may be a valuable antiarrhythmic pharmacotherapeutic strategy for AF.

KEYWORDS

antiarrhythmic drugs, atrial fibrillation, computational modeling, population-based modeling, quantitative Systems Pharmacology, reverse rate dependence

Abbreviations: 1D, one dimensional; AF, atrial fibrillation; AP, action potential; APD_{xx} , action potential duration at xx% of repolarization; B, coefficient; CV, conduction velocity; CZ, Colman-Zhang model; ERP, effective refractory period; GB, Grandi-Bers model; I_{KACh} , the ACh activated inward rectifier K^+ current; I_{K2P} , the $K_{2P3.1}$ 2-pore-domain K^+ current; I_{KCa} , the small conductance Ca^{2+} -activated K^+ current; I_{Kr} , the rapid delayed rectifier K^+ current; I_{Kur} , the ultra-rapid delayed rectifier K^+ current; I_{Na} , fast Na^+ current; nSR, normal sinus rhythm; RD, rate dependence; RMP, resting membrane potential; RR, repolarization reserve; WL_{λ} , wavelength.

1 | INTRODUCTION

The development of effective and safe pharmacotherapy for treatment of atrial fibrillation (AF), the most common cardiac arrhythmia, remains an important unmet clinical need. This is partly due to limited efficacy and undesired side effects of available pharmacotherapies, including an increased risk for lethal ventricular arrhythmias (Yap & Camm, 2003). Atrial-predominant K^+ currents, including the **ultra-rapid delayed rectifier K^+ current**, I_{Kur} , the **small conductance Ca^{2+} -activated K^+ current**, I_{KCa} , the **$K_{2p3.1}$ 2-pore-domain K^+ current**, I_{K2P} , and the **acetylcholine-activated inward rectifier K^+ current**, I_{KACh} , are attractive targets for AF pharmacotherapy, in that their modulation may enable antiarrhythmic effects without disturbing normal ventricular function. Selectively blocking any one of these currents has been proposed as a novel approach to anti-AF pharmacotherapy (Hancox, James, Marrion, Zhang, & Thomas, 2016; Peyronnet & Ravens, 2019; Voigt & Dobrev, 2016). Additionally, combination therapy may reduce deleterious side effects (Calvo, Filgueiras-Rama, & Jalife, 2018), by allowing synergistic antiarrhythmic drug responses and thus reducing therapeutic doses. Recently, there has been a growing interest in exploring and utilizing synergistic antiarrhythmic effects of multi-channel or multi-compound blockade schemes (Aguilar, Xiong, Qi, Comtois, & Nattel, 2015; Kirchhoff, Goldin Diness, Sheykhzade, Grunnet, & Jespersen, 2015; Ni et al., 2017; Reiffel et al., 2015) for terminating AF. Yet it is not known whether combined inhibition of multiple atrial-predominant currents can render beneficial synergistic anti-AF effects in the atria. Further, it is well known that K^+ channel blockers/class III antiarrhythmic drugs exhibit reverse (negative) rate dependence (RD) (So, Hu, Backx, Puglisi, & Dorian, 2006; Virág et al., 2009; Wang, Pelletier, Talajic, & Nattel, 1990), that is, greater action potential (AP) duration (APD) lengthening at slow versus fast pacing rates. However, as AF is characterized by rapid and irregular atrial activations, antiarrhythmic drugs exhibiting positive rate dependence are preferable. Compounds should display potent antiarrhythmic effects at fast rates (efficacy) and minimize side effects at slow rates (safety). It remains unknown how combined blockade of atrial-predominant K^+ currents modulates rate dependence of action potential duration changes.

Quantitative Systems Pharmacology approaches have been successfully employed to dissect arrhythmia mechanisms (Bers & Grandi, 2011) and quantitatively predict complex responses of cardiac electrophysiology to various forms of drug modulation (Aguilar et al., 2015; Cummins, Dalal, Bugana, Severi, & Sobie, 2014; Ellinwood, Dobrev, Morotti, & Grandi, 2017b, 2017a; Grandi, Dobrev, & Heijman, 2019; Grandi & Maleckar, 2016; Morotti, McCulloch, Bers, Edwards, & Grandi, 2016; Ni et al., 2017; Ni, Zhang, Grandi, Narayan, & Giles, 2019). These methods provide integrative frameworks to complement preclinical studies seeking to optimize antiarrhythmic therapy. Furthermore, given variable drug efficacy and susceptibility to side effects, population-based computational approaches have proven valuable for understanding inter-subject variability in electrophysiological properties and cardiotoxicity (Cummins et al., 2014; Morotti & Grandi, 2017; Ni, Morotti, & Grandi, 2018; Passini et al., 2017; Sarkar & Sobie, 2011;

What is already known

- Current pharmacological therapeutic strategies for atrial fibrillation (AF) remain unsatisfactory.
- Atrial-predominant current block has been proposed as a promising anti-AF strategy.

What this study adds

- Combined block of multiple atrial-predominant K^+ currents promotes synergistic prolongation of action potential and refractoriness.
- This synergy displays favourable positive rate dependence (fast-rate selectivity) and dose dependence.

What is the clinical significance

- Combined multiple atrial-predominant K^+ -current blockade may be a valuable anti-AF strategy.

Sobie, 2009). These methods are especially useful in AF, which is characterized by various degrees of AF-associated remodelling and a multitude of mechanisms and aetiologies.

Here, we developed a novel Quantitative Systems Pharmacology framework to simulate and quantitatively assess synergistic anti-AF effects on human atrial biomarkers obtained when blocking multiple atrial-predominant K^+ currents simultaneously. A general workflow is illustrated in the Supporting Information. We have simulated virtual populations of human atrial myocytes and one-dimensional tissue strands to quantify effects of blocking three atrial-predominant currents (I_{Kur} , I_{KCa} and I_{K2P}) on atrial action potential duration and excitation wavelength (WL). We apply sensitivity analyses of AP biomarkers and atrial repolarization reserve (RR) to understand the interactions and rate dependence of multicurrent block in affecting these outcomes. Finally, we perform population-based simulations of current block to confirm synergistic effects of multicurrent block that exhibit positive rate dependence. Our results show that simultaneous inhibition of atrial-predominant K^+ currents leads to significant synergy (i.e. greater than additive effects) in action potential duration and wavelength prolongation, especially at fast atrial rates (as in AF), suggesting that this poly-therapy may be a valuable strategy for anti-AF pharmacotherapy.

2 | METHODS

2.1 | Models

To simulate human atrial myocyte electrophysiology, we employed our previously developed computational models: Colman-Zhang model (CZ, Colman et al., 2013) with recent updates (Ni et al., 2017; Ni et al., 2019) and Grandi-Bers model (GB, Grandi et al., 2011) with

updates (Ellinwood et al., 2017a, 2017b; Morotti et al., 2016). These two models represent distinct morphological subtypes of human atrial AP (Wang, Fermini, & Nattel, 1993): Colman–Zhang model displays a type-1 AP with notch-and-dome morphology and a pronounced plateau phase, whereas Grandi–Bers model simulates a type-3 AP with typical triangular shape. We included formulations of I_{KCa} and I_{K2P} in both atrial models, adapted from Skibsbjerg et al. (2016) and Schmidt et al. (2015), respectively.

2.2 | Generation and calibration of populations of models

We first created normal sinus rhythm populations by randomly perturbing transmembrane ionic current and transporter parameters of Colman–Zhang and Grandi–Bers baseline models (Table 1) using the approach proposed by Sobie (2009). Specifically, in both models, each maximum conductance and transport rate parameter was allowed to vary independently according to a log-normal distribution. We chose $\sigma = 0.2$ based on previous studies (Ellinwood et al., 2017a; Morotti & Grandi, 2017; Sobie, 2009) to cover a range of variability similar to that seen in experiments, while limiting the number of non-physiological model variants to be excluded upon calibration. A workflow and details on the generation and size of each normal sinus rhythm and AF population are given in Supporting Information.

We used experimental AP biomarkers to calibrate the model populations (Britton et al., 2013; Muszkiewicz et al., 2016) by excluding the model variants in which simulated biomarkers were outside the experimentally observed range reported by Ravens et al. (2014). Specifically, we compared action potential duration measured at 90% and 50% repolarization, APD_{90} , APD_{50} and resting membrane potential (RMP) of each virtual cell (steady-state values at 1 Hz pacing) with those experimentally measured in Ravens et al. (2014). Model variants were excluded if any biomarker was found differing more than 3 SDs from the experimental mean (Figure 1a,c). Additionally, we removed virtual cells displaying abnormal resting membrane potentials (same constraints as 1 Hz in the absence of resting membrane potential measurements at 3 Hz from the same source) when paced at 3 Hz.

Starting from the accepted normal sinus rhythm model variants, we further created populations of virtual atrial cells with AF-induced cellular remodelling effects. We simulated AF-induced remodelling of atrial electrophysiology as described in previous studies (Colman–Zhang model as in Colman et al., 2013; Colman, Ni, Liang, Schmitt, & Zhang, 2017; Ni et al., 2017, and Grandi–Bers model as in Grandi et al., 2011). In addition to these well-established models of AF-remodelling, we considered various, sometimes contradictory, reported alterations of I_{Kur} , I_{KCa} and I_{K2P} in AF myocytes from published experimental studies. Indeed, while several studies showed no AF-associated changes in I_{Kur} (Bosch et al., 1999; Grammer, Bosch,

TABLE 1 Glossary for human atrial model parameters that were perturbed for constructing populations of atrial models

Parameter	Model		Note
	CZ	GB	
G_{Na}^a	✓	✓	Fast sodium current, maximal conductance
G_{NaL}^b	✓	N/A	Late component of sodium current, maximal conductance
G_{CaL}	✓	✓	L-type calcium current, maximal conductance
G_{to}	✓	✓	Transient outward current, maximal conductance
G_{Kur}	✓	✓	Ultra-rapid delayed rectifier potassium current, maximal conductance
G_{Kr}	✓	✓	Rapid delayed rectifier potassium current, maximal conductance
G_{Ks}	✓	✓	Slow delayed rectifier potassium current, maximal conductance
G_{K1}	✓	✓	Inward rectifier potassium current, maximal conductance
G_{KCa}	✓	✓	Small-conductance calcium-activated potassium current, maximal conductance
G_{K2P}	✓	✓	$K_{2P3.1}$ 2-pore-domain potassium current, maximal conductance
G_{NaCa}	✓	✓	Sodium/calcium exchange current, maximal exchange rate
G_{NaK}	✓	✓	Sodium/potassium pump current, maximal pump rate
G_{bNa}	✓	✓	Background sodium current, maximal conductance
G_{bCa}	✓	✓	Background calcium current, maximal conductance
G_{CaP}	✓	✓	Sarcoplasmic calcium pump current, maximal pump rate
G_{ClCa}^c	N/A	✓	Calcium activated chloride current, maximal conductance
G_{ClB}^c	N/A	✓	Background chloride current, maximal conductance

^aIn Grandi–Bers (GB) model, the fast Na^+ current was described using a Markov formulation as in Morotti et al., 2016 and thus changing G_{Na} depicts scaling of both fast and slow components of Na^+ current.

^bIn Colman–Zhang model (CZ), G_{NaL} describes the late component of the Na^+ current, which was modelled independently of the fast inactivating component.

^cTwo Cl^- currents are present in GB but not CZ model: background (I_{ClB}) and Ca^{2+} activated (I_{ClCa}) Cl^- current.

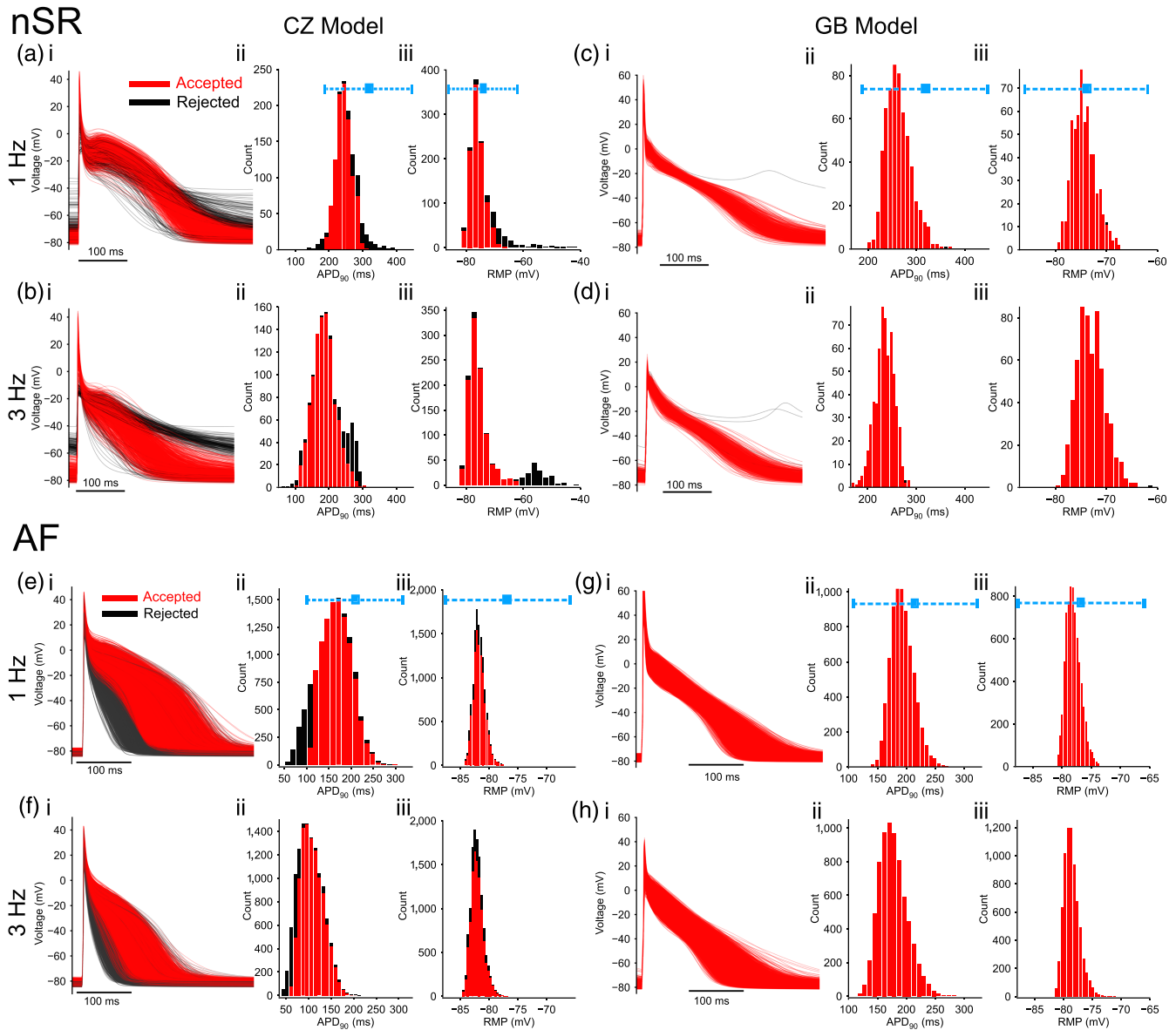


FIGURE 1 Simulated action potentials (APs) for human atrial myocyte populations. (a–d) normal sinus rhythm (nSR) populations. (e–h) AF populations. Myocytes were paced at 1 Hz (panels a, c and e, g) and 3 Hz (panels b, d and f, h). The left panels (a, b, e, f) show data for Colman–Zhang (CZ) model while results from Grandi–Bers (GB) model are plotted on the right (c, d, g, h). In each panel, column (i) superimposed APs of the atrial populations; column (ii) and (iii) distribution of action potential duration and resting membrane potential, respectively. Action potential duration was measured at 90% repolarization (APD_{90}). Rejected model variants following experimental data calibration are indicated in black. Ranges of experimental measurements (mean $\pm 3 \times$ SD) are indicated in blue symbols and bars

Kühlkamp, & Seipel, 2000; Workman, Kane, & Rankin, 2001), significant reductions in this current have also been well-documented (Caballero et al., 2010; Gonzalez de la Fuente et al., 2012; Wagoner, Pond, McCarthy, Trimmer, & Nerbonne, 1997). Similarly, I_{KCa} was found increased following burst pacing (Ozgen et al., 2007) or atrial tachypacing (Qi et al., 2014) but decreased in myocytes from AF patients (Skibsbjerg et al., 2014). Further, AF substantially enhances the activity of I_{K2P} (Schmidt et al., 2015, 2017), but this increase is mitigated in the presence of left ventricular dysfunction (Schmidt et al., 2017). To address the complexity and variability in AF

remodelling collectively revealed by these studies, which could affect the atrial response when targeting I_{Kur} , I_{KCa} and I_{K2P} , we considered various possible permutations of reported AF-remodelling effects on each of the three currents (Table S1).

Lastly, to calibrate the AF-model populations we compared the AP biomarkers (steady-state APD_{90} , APD_{50} , and resting membrane potential values at 1 Hz pacing) to those measured in atrial myocytes from AF patients (Ravens et al., 2014). Again, models exhibiting biomarkers more than 3 SDs from the experimental mean were excluded.

2.3 | Simulations of atrial-predominant K⁺ current blockade in AF

We simulated blockade of the atrial-predominant K⁺ currents with a simple pore block scheme (Yuan, Bai, Luo, Wang, & Zhang, 2015) (i.e. only changing maximum current conductance) and evaluated effects of 50% block of I_{Kur}, I_{KCa}, and/or I_{K2P} on the virtual atrial myocytes in AF. When quantifying the effects of current block, we chose APD₉₀ as a biomarker that closely relates to refractoriness and is frequently quantified in investigations of class III antiarrhythmic drugs. For simplicity, we denote APD₉₀ as action potential duration unless otherwise specified. We determined the interaction between effects of multcurrent block on action potential duration and defined synergy for combined effects being greater than additive sum of separate effects and antagonism for less-than-additive effects.

Two frequencies (1 and 3 Hz) are chosen as low and high to evaluate the effect of current block during normal sinus rhythm and fast atrial rate. We did not simulate faster atrial rates to avoid the frequent occurrence of action potential duration alternans seen in atria of AF patients (Narayan, Franz, Clopton, Pruvot, & Krummen, 2011), which would have prevented meaningful assessment of action potential duration prolongation. Accordingly, upon data analysis, we also excluded model variants exhibiting alternans of beat-to-beat APD₉₀ variation greater than 5 ms in either the baseline or blockade conditions.

To assess whether our results depend on the extent of current blockade, we modelled additional percentages of current blockade (25%, 75% and 100%). Considering the substantial computational cost, we selected two subpopulations (#1 and #5 in Table S1). In these two subpopulations, I_{Kur} was reduced by 50% and I_{K2P} increased by threefold accounting for AF-remodelling, following the AF parameterizations in previous modelling studies (Colman et al., 2013; Ellinwood et al., 2017a; Grandi et al., 2011; Ni et al., 2017); we considered two different effects of AF-remodelling on I_{KCa}, a 50% reduction in #1 and twofold increase in #5 to cover the different observations from Ozgen et al. (2007), Qi et al. (2014), and Skibsbbye et al. (2014).

2.4 | One-dimensional strand models of human atrial tissue

We constructed one-dimensional (1D) models of human atrial strands to evaluate the responses of the action potential duration (APD), effective refractory period (ERP), conduction velocity (CV) and wavelength (WL) to K⁺ current blockade in tissue. Considering the substantial computational cost of performing simulations of populations of tissues, we limited one dimensional simulations to Colman–Zhang model (less computationally expensive to solve than Grandi–Bers model) and selected AF subpopulations (#1 and #5 as above). We anticipate differences between Colman–Zhang and Grandi–Bers model in one dimensional simulations would be consistent with those seen at the single-cell level. To understand whether AF-induced changes in cell–cell coupling, for example, due to fibrosis (Burstein & Nattel, 2008), affect the tissue responses to current block, we

considered both normal and 40% reduced tissue conductivity. The resulting conduction velocity of 0.62 versus 0.46 m·s⁻¹, respectively (Table S6) was comparable to that seen in normal and remodelled atrial tissue (Hansson et al., 1998; Krul et al., 2015).

2.5 | Sensitivity analysis

To study the sensitivity of action potential duration and current block-induced action potential duration change to model parameters, we performed multivariable linear regression, as detailed in previous studies by Dr Sobie's group (Cummins et al., 2014; Sarkar & Sobie, 2011; Sobie, 2009). Parameter sensitivity of action potential duration predicts effects of blocking ionic currents on action potential duration: If the sensitivity coefficient (**B**) is positive, current block would shorten action potential duration, and if negative, inhibiting this current would prolong action potential duration.

Sensitivity analysis of action potential duration can also shed light on rate dependence of action potential duration changes through comparing the sensitivity coefficients between fast and slow pacing rates (Cummins et al., 2014). Here, to quantitatively assess rate dependence of action potential duration modulation when blocking the atrial-predominant K⁺ currents (I_{K2P}, I_{KCa}, and I_{Kur}), for each model parameter, we define rate dependence coefficients (**B**_{RD}) as the weighted difference between the sensitivity coefficients of 1 Hz (**B**₁) and 3 Hz (**B**₃) groups (**B**_{RD} = **B**₁ – **B**₃) (see details for scaling and comparing sensitivity coefficients in Supporting Information). As such, a positive **B**_{RD} (i.e. **B**₁ > **B**₃) indicates a decrease in the model parameter (e.g. by current block) will lengthen action potential duration more at fast than slow pacing rate (i.e. ΔAPD_{fast} > ΔAPD_{slow}) and thus is associated with positive rate dependence. Similarly, a negative **B**_{RD} suggests negative rate-dependent action potential duration modulation when inhibiting the underlying ionic current.

Further, sensitivity analysis can be applied to understand modulations by ionic parameters of repolarization reserve (RR), a concept describing the prevention of excessive action potential duration lengthening subsequent to inhibiting one repolarizing current through compensation by other repolarizing currents (Varró & Baczkó, 2011). This procedure requires quantification of repolarization reserve, which can be derived from action potential duration change following block of a current (Sarkar & Sobie, 2011). Here, we extended sensitivity analysis of repolarization reserve to identify interactions among ion channel modulators. We derived three quantitative descriptions of the repolarization reserve using our simulated data of atrial populations before and after block of either of I_{K2P}, I_{KCa}, or I_{Kur}. Specifically, in a population of atrial cells, the repolarization reserve (RR) of each cell derived from simulated block of current X (RR_X) was calculated as

$$RR_X = \frac{APD_{Block-free}}{APD_{X\ block}},$$

where X represents either I_{K2P}, I_{KCa}, or I_{Kur}. APD_{Block-free} is the action potential duration rate dependence of the cell in the absence of the

block at current I_X , and $APD_{X \text{ block}}$ is the action potential duration after I_X block. Hence, a greater value of RR_X indicates stronger repolarization reserve of the cell and vice versa. If all RR_X values for the population were then used as the dependent variable (as for action potential duration previously) in a sensitivity analysis, the fitted coefficients indicate how each current in the model affects repolarization reserve (during simultaneous block of I_X): A negative sensitivity coefficient indicates that decreasing a given current would enhance the repolarization reserve, whereas a positive coefficient suggests that reducing the current would impair the repolarization reserve. Therefore, for a given current (I_Y), a negative sensitivity coefficient indicates that a reduction (e.g., block) of I_Y in the cell can enhance its repolarization reserve (greater RR_X thus smaller $\frac{APD_{X \text{ block}}}{APD_{\text{Block-free}}}$ or lower action potential duration prolongation). In other words, in the presence of I_Y block the action potential duration prolongation due to I_X block is reduced, suggesting competition/antagonism between blocking I_Y and I_X in lengthening the action potential duration. Conversely, a positive coefficient indicates that blocking I_Y would impair repolarization reserve and exaggerate the action potential duration prolongation caused by blocking I_X , thus indicating the presence of synergy between block of I_Y and I_X in lengthening the action potential duration.

2.6 | Data and statistical analysis

We applied the non-parametric bootstrap method to characterize the rate dependence of action potential duration (and other tissue-level biomarkers) changes and interactions of multiple channel blockades, as detailed in the Supporting Information - Supporting Methods. Specifically, the RD of APD change was deemed positive if the lower limit of the confidence interval (CI) for the median of $\Delta APD_{3\text{Hz}} - \Delta APD_{1\text{Hz}}$ is > 0 , and negative if the upper limit of CI is < 0 . Potential interactions were assessed by comparing changes due to combined block and the sum of the effects of each individual current block. Using again APD as an example, the interaction between I_{K2P} and I_{Kur} block is calculated as

$$\text{Interaction}_{K2P+Kur} = \Delta APD_{K2P+Kur \text{ block}} - (\Delta APD_{K2P \text{ block}} + \Delta APD_{Kur \text{ block}}) \quad (1)$$

where for each current block, $\Delta APD_{X \text{ block}} = \frac{APD_{X \text{ block}} - APD_{\text{Block-free}}}{APD_{\text{Block-free}}} \times 100(\%)$. Hence, an interaction exists if the CI for the median $\text{Interaction}_{K2P+Kur}$ does not contain 0, and is deemed synergistic if the lower limit of CI is > 0 and antagonistic if the upper limit of CI is < 0 . CIs were obtained with confidence levels set to 95% with Bonferroni-type correction for each group of analysis (i.e., considering 7 comparisons for RD characterizations and 4 comparisons/combinations for interactions for each subpopulation). The data and statistical analysis comply with the recommendations of the *British Journal of Pharmacology* on experimental design and analysis in pharmacology (Curtis et al., 2018).

2.7 | Software availability

Details on software and numerical methods are in the Supporting Information. Source code and documentation are freely available at <http://elegrandi.wixsite.com/grandilab/downloads> and <https://github.com/drgrandilab>.

2.8 | Nomenclature of targets and ligands

Key protein targets and ligands in this article are hyperlinked to corresponding entries in <http://www.guidetopharmacology.org>, the common portal for data from the IUPHAR/BPS Guide to PHARMACOLOGY (Harding et al., 2018) and are permanently archived in the Concise Guide to PHARMACOLOGY 2019/20 (Alexander et al., 2019).

3 | RESULTS

3.1 | Calibrated populations of simulated myocytes under normal sinus rhythm and AF conditions

We utilized our well-established models of human atrial AP and Ca^{2+} handling, Colman-Zhang (CZ, Colman et al., 2013) and Grandi-Bers (GB, Grandi et al., 2011) to generate populations of atrial cell model variants in normal sinus rhythm (Figure 1a-d). Distributions of action potential duration and resting membrane potential for the simulated atrial populations at both 1 and 3 Hz following calibration with experimentally measured action potential duration (APD) and resting membrane potential data from (Ravens et al., 2014) are in Table S2. By incorporating AF-remodelling effects into the normal sinus rhythm variants, we obtained 12 AF-subpopulations including variable sign and degree of remodelling on I_{K2P} , I_{KCa} and I_{Kur} (Table S1), reflecting the variability in reported AF-remodelling effects on these currents. APD_{50} , APD_{90} and resting membrane potential distributions for the aggregate AF population and each of these 12 subpopulations were then calibrated to the experimental data from (Ravens et al., 2014) (Figure 1e-h) and are shown in Tables S2 and S3, respectively.

3.2 | Sensitivity analysis revealed rate dependence of APD modulation

Rate-dependent action potential duration modulation is an important property of class III antiarrhythmic drugs, which often present unfavourable reverse (negative) rate dependence (So et al., 2006; Virág et al., 2009; Wang et al., 1990). A previous study demonstrated that sensitivity analysis of action potential duration provides insights into rate dependence of ventricular action potential duration changes following alterations in ionic currents (Cummins et al., 2014). We applied sensitivity analysis to predict rate dependence of action potential duration changes when blocking these atrial-predominant K^+

currents (Figure 2 and Figure S1). First, we used multivariable linear regression analysis to calculate action potential duration sensitivity coefficients (Sobie, 2009), which, as might be anticipated, were generally negative for $G_{K_{Kur}}$, $G_{K_{Ca}}$ and $G_{K_{2P}}$ (Figure 2a,c,e,g), suggesting that block of these currents would tend to prolong action potential duration, with the exception of $I_{K_{Kur}}$ in the Grandi-Bers model population at 1 Hz. Then, comparing the sensitivity coefficients of slow versus fast pacing rate, we derived rate dependence coefficients (B_{RD} , as described in Section 2). Positive B_{RD} indicates that current blockade causes greater action potential duration prolongation at fast versus slow rates, that is positive rate dependence, and vice versa. Analysis of B_{RD} (Figure 2b,d) revealed that, in normal sinus rhythm myocyte

simulations, inhibiting $I_{K_{Kur}}$ produces positive rate dependence in action potential duration prolongation for both model populations, whereas $I_{K_{2P}}$ block favours positive rate dependence in Colman-Zhang model but not Grandi-Bers model population. In AF, B_{RD} (Figure 2h) for $G_{K_{Kur}}$, $G_{K_{Ca}}$, and $G_{K_{2P}}$ for the Grandi-Bers model populations were positive, suggesting that inhibiting these currents would produce positive rate dependence of action potential duration prolongation. In contrast, in Colman-Zhang model populations (Figure 2f), positive B_{RD} was seen for $G_{K_{Kur}}$ only, indicating that $I_{K_{Kur}}$ block is associated with positive, but $I_{K_{Ca}}$ and $I_{K_{2P}}$ inhibition with negative rate dependence of action potential duration change.

3.3 | Simulations of K^+ -current block validated predicted rate dependence

Focusing our subsequent analyses on the AF model populations, we simulated effects of blocking atrial-predominant K^+ currents ($I_{K_{Kur}}$, $I_{K_{Ca}}$, and $I_{K_{2P}}$) to verify the rate dependence of action potential duration modulation predicted by the sensitivity analysis (B_{RD}) when each current is blocked and assessed rate dependence of action potential duration changes when multiple currents are inhibited in combination. Qualitative assessment of AP traces (Figure 3 and Figure S2) reveals that $I_{K_{2P}}$ block modified both phase 2 and 3 of the AP (Figure 3a), whereas $I_{K_{Ca}}$ block predominantly affected phase 3 (Figure 3b) and $I_{K_{Kur}}$ mostly impacted phase 2 (Figure 3c). Both phase 2 and phase 3 changes were seen in multicurrent block simulations (Figure 3d–g). For quantitative assessment, we calculated both absolute and fractional action potential duration changes due to block of each individual K^+ current (Figure 4a–d, first three columns), paired block (Figure 4a–d, fourth to sixth column) and combined block of all three currents (Figure 4a–d, last column) at 1 and 3 Hz (Figure 4a,c and Figure 4b,d, respectively, and Table S4). Notably, simulations generally predicted action potential duration prolongation, with the exception of a substantial fraction of Grandi-Bers model variants in which $I_{K_{Kur}}$ block alone or combined with $I_{K_{Ca}}$ block shortened action potential duration at 1-Hz pacing (Figure 3c, ii and f, ii, Figure 4a,c and

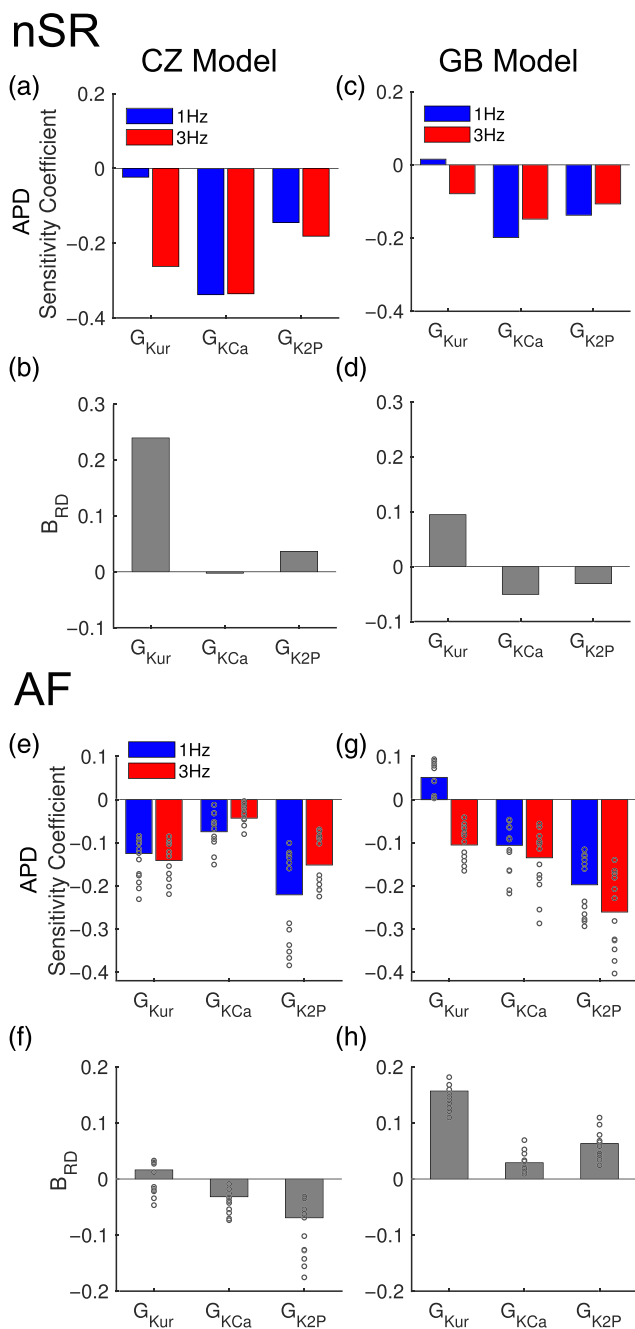


FIGURE 2 Sensitivities of action potential duration and rate-dependent action potential duration modulation for atrial-predominant K^+ parameter ($G_{K_{Kur}}$, $G_{K_{2P}}$, and $G_{K_{Ca}}$). We applied multivariable linear regression to virtual atrial (a–d) normal sinus rhythm (nSR) and (e–h) AF myocyte populations. (a, c, e, g) Sensitivity coefficients of action potential duration to perturbations of three parameters of interest ($G_{K_{Kur}}$, $G_{K_{Ca}}$ and $G_{K_{2P}}$) for myocytes paced at 1 and 3 Hz. (b, d, f, h) action potential duration (APD) rate-dependence (RD) coefficients (B_{RD}) for these currents. Positive B_{RD} indicates inhibition of this current favours producing positive rate dependence of action potential duration prolongation and vice versa. In (e–h), results for each AF subpopulation are plotted as open circles and those for the aggregate dataset are represented by bar plots. For the 12 AF-subpopulations, the variability in AF-remodelling effects caused variations in sensitivity coefficients. Results of the sensitivity analysis for the full set of model parameters varied in simulations are shown in Figure S1

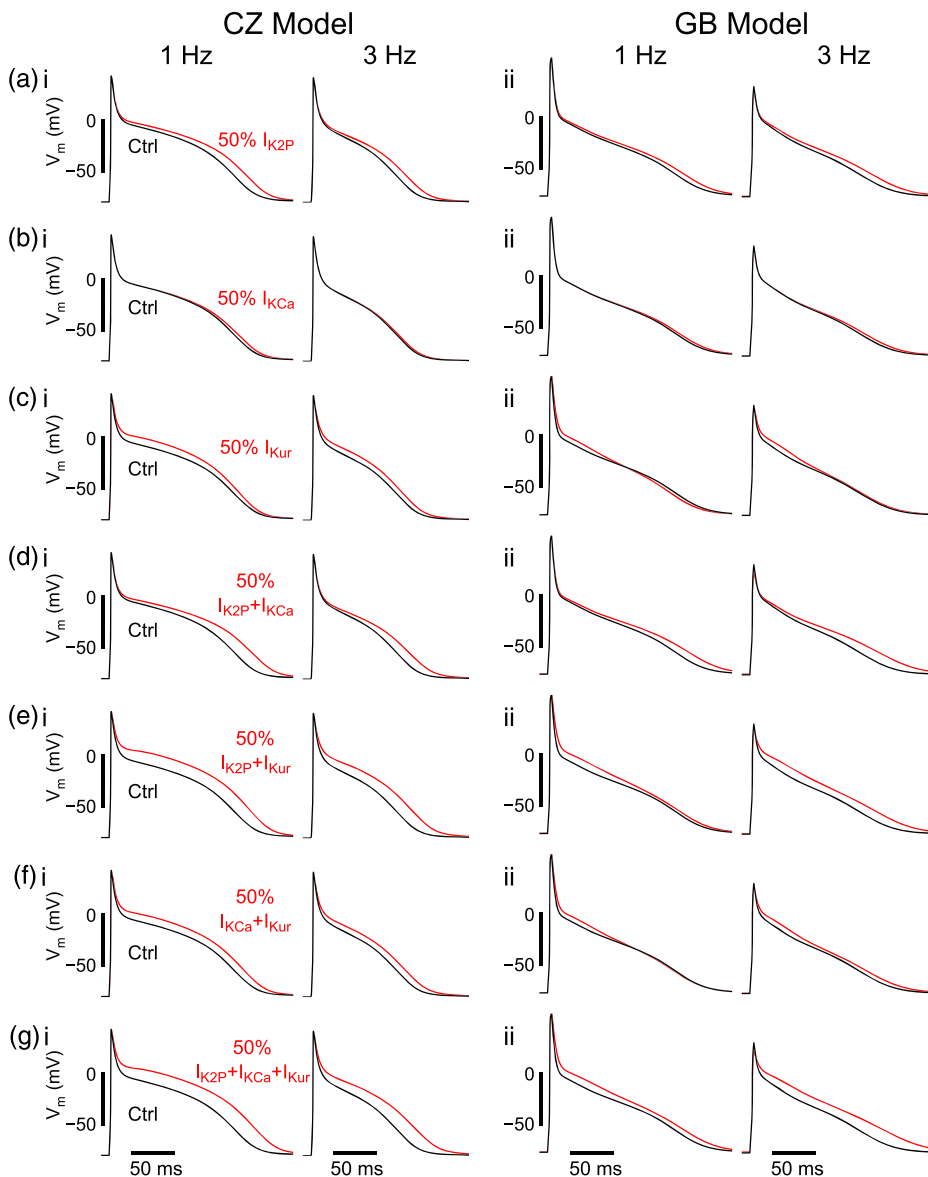


FIGURE 3 Action potential (AP) waveform changes due to block of atrial-predominant K^+ currents. Example of AP modulations at 1 and 3 Hz following various regimens concerning 50% block of I_{K2P} , I_{KCa} and I_{Kur} . Each row depicts APs with/without 50% block of (a) I_{K2P} , (b) I_{KCa} , (c) I_{Kur} , (d) $I_{K2P} + I_{KCa}$, (e) $I_{K2P} + I_{Kur}$, (f) $I_{KCa} + I_{Kur}$ and (g) $I_{K2P} + I_{KCa} + I_{Kur}$ from simulations with (left columns) Colman-Zhang model (CZ; subpopulation #5, variant #310) and (right columns) Grandi-Bers (GB) models (subpopulation #5, variant #287)

Table S4). Note that these results agree well with the predictions from the sensitivity analysis, with negative coefficients (associated with action potential duration prolongation) for all atrial-predominant K^+ conductances except for G_{Kur} at 1 Hz in Grandi-Bers model population (Figure 2e,g). Overall, individual current block produced minor to moderate effects on action potential duration; I_{K2P} block caused greater Δ APD than either I_{Kur} or I_{KCa} block, consistent with previous experimental studies on effects of I_{K2P} (Schmidt et al., 2015), I_{Kur} (Ford et al., 2016), and I_{KCa} (Skibsbjerg et al., 2014) block.

To describe the rate dependence of Δ APD upon atrial-predominant K^+ -current block, we applied bootstrap analysis to estimate CIs of median difference Δ APD for fast versus slow pacing rate as described in Section 2 (Figure S3). The analysis showed that action potential duration prolongation due to blocking I_{Kur} in both Colman-Zhang and Grandi-Bers model populations exhibited positive rate dependence (highlighted in black bars, Figure 4a,c), in agreement with positive sensitivity coefficients B_{RD} (Figure 2f,h). Interestingly, this

favourable positive rate dependence of action potential duration modulation has been reported for XEN-D0103 (Ford et al., 2016), a selective I_{Kur} blocker. In the Grandi-Bers model population, positive rate dependence was found upon blocking each current individually, and also seen in multicurrent block (Figure 4c,d, Table S4). In Colman-Zhang model simulations, negative rate dependence was predominantly found in absolute Δ APD, but positive rate dependence was found in fractional Δ APD (Figure 4a,b). This discrepancy could be explained by shorter baseline (drug-free) action potential duration at 3 Hz versus 1 Hz (Figure 1e,ii and f,ii). Multicurrent block generally produced stronger positive rate dependence than individual current block, especially when I_{Kur} , I_{K2P} and I_{KCa} were all blocked simultaneously (Figure 4b,d and Figure S3). Collectively, these results verified predictions from our sensitivity analyses and show that multi-atrial-predominant K^+ -current block promoted positive rate dependence of action potential duration modulation, a favourable property for class III antiarrhythmics.

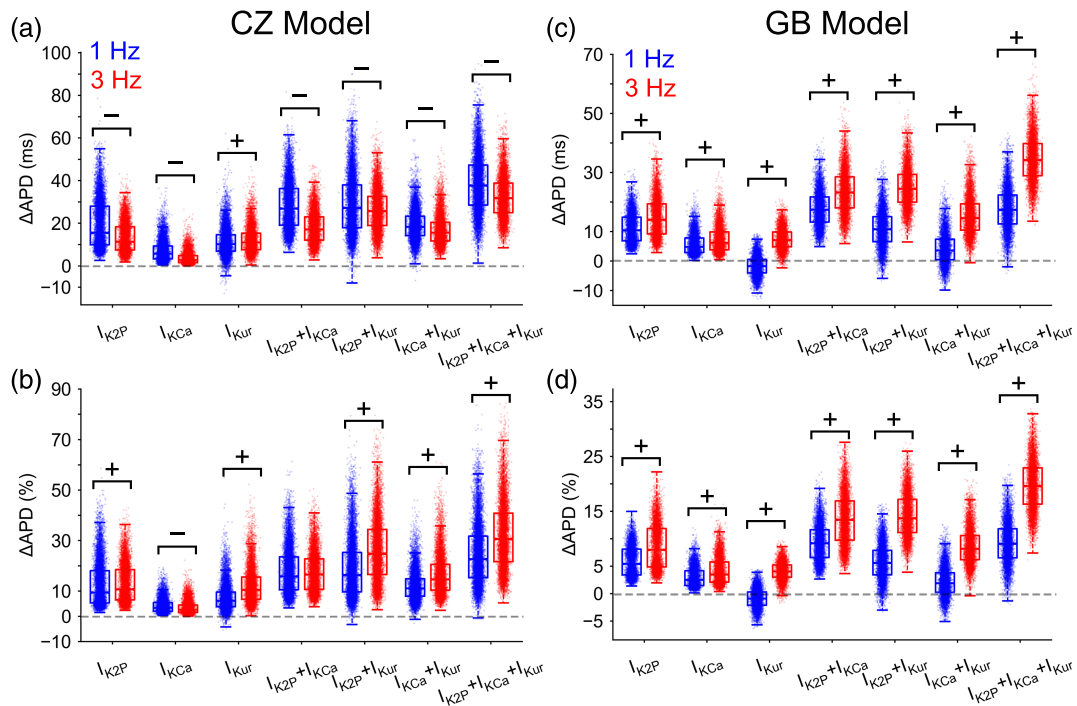


FIGURE 4 Effects of 50% block of I_{K2P} , I_{KCa} or I_{Kur} on action potential duration in AF-remodelled atrial populations at slow and fast pacing rates. In these simulations, three atrial-predominant- K^+ currents are partially (50%) inhibited individually or in combination during pacing at 1 Hz (blue) and 3 Hz (red). (a, b) Simulation results for Colman-Zhang model (CZ) population. (c, d) Results obtained from Grandi-Bers model (GB) population. The top (a, c) and bottom (b, d) panels illustrate absolute and fractional action potential duration changes, respectively. The sign of ΔAPD (action potential duration) rate dependence (RD) from confidence interval analysis (Figure S3) is indicated as follows: “+” for positive RD and “-” for negative RD

3.4 | Sensitivity analysis of atrial repolarization reserve revealed synergistic APD prolongation

Repolarization reserve refers to the concept that when one repolarizing current is inhibited other repolarizing currents may compensate and prevent excessive action potential duration lengthening (Varró & Baczkó, 2011). Here, we define atrial repolarization reserve as the ratio of block-free action potential duration to action potential duration upon K^+ -current block and apply sensitivity analysis of repolarization reserve to uncover interactions among multicurrent blockade in modulating action potential duration (see Section 2). In Figure 5a, we calculated repolarization reserve as $\frac{APD_{Block-free}}{APD_{IK2P\ block}}$. Blocking currents associated with negative sensitivity coefficients can enhance repolarization reserve through increasing $\frac{APD_{Block-free}}{APD_{IK2P\ block}}$, thus suggesting a competition/antagonistic effect between blocking this current and I_{K2P} in prolonging the action potential duration. Conversely, if a current is associated with a positive sensitivity coefficient, blocking this current is expected to synergistically interact with I_{K2P} block in lengthening the action potential duration. In the Colman-Zhang model population, the negative sensitivity coefficient for G_{Kur} at 1 Hz shifted towards positive at 3 Hz (Figure 5ai), suggesting that inhibition of I_{Kur} would compete against I_{K2P} block in lengthening action potential duration at 1 Hz and this was diminished at 3 Hz. Consistently, positive sensitivity coefficients were seen for G_{KCa} in the Colman-Zhang

model population and both G_{Kur} and G_{KCa} in the Grandi-Bers model population (Figure 5a, i-ii), suggesting synergistic effects in action potential duration prolongation for $I_{Kur} + I_{K2P}$ or $I_{KCa} + I_{K2P}$ block. Given our definition of repolarization reserve, large coefficients were associated with the current being blocked (I_{K2P} in Figure 5a, I_{KCa} in Figure 5b, and I_{Kur} in Figure 5c), as also shown in Sarkar and Sobie (2011).

Similarly, applying sensitivity analysis to repolarization reserve computed as $\frac{APD_{Block-free}}{APD_{IKCa\ block}}$, positive coefficients for G_{Kur} and G_{K2P} in both populations indicated potential synergy in lengthening action potential duration for $I_{Kur} + I_{KCa}$ or $I_{K2P} + I_{KCa}$ block (Figure 5b). Further, sensitivity analysis of repolarization reserve measured as $\frac{APD_{Block-free}}{APD_{IKur\ block}}$ (Figure 5c) revealed interactions in $I_{Kur} + I_{K2P}$ and $I_{Kur} + I_{KCa}$ block consistent with the analyses above (Figure 5a,b): the sensitivity coefficient for G_{K2P} was negative at 1 Hz and shifted towards positive at 3 Hz in the Colman-Zhang model populations; positive coefficients were seen for G_{KCa} in both Colman-Zhang and Grandi-Bers model populations and for G_{K2P} in Grandi-Bers model population. Further, the coefficient for G_{Kur} itself was positive at 1 Hz for the Grandi-Bers model population (Figure 5c, ii), which indicates that increasing G_{Kur} would result in greater $\frac{APD_{Block-free}}{APD_{IKur\ block}}$ and thus less action potential duration prolongation, in agreement with the observation that I_{Kur} block shortened action potential duration (Figure 4c). Interestingly, coefficients for G_{Kr} were positive across pacing rates and Colman-Zhang

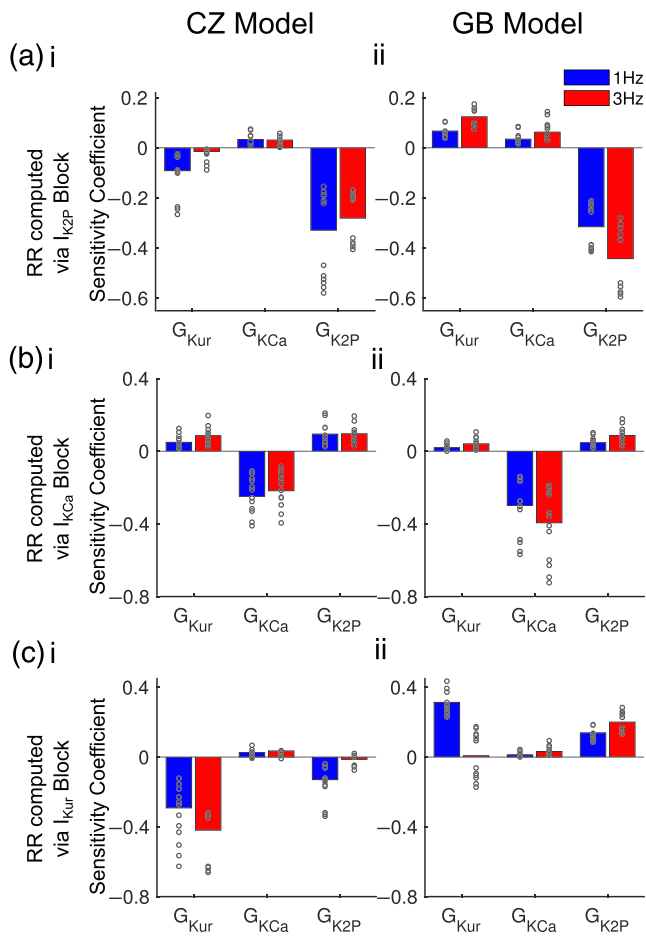


FIGURE 5 Parameter sensitivity of repolarization reserve (RR) for $G_{K_{ur}}$, $G_{K_{Ca}}$ and $G_{K_{2P}}$. (a–c) Sensitivity coefficients of repolarization reserve derived from the ratio between action potential durations before and after 50% block of (a) $I_{K_{2P}}$, (b) $I_{K_{Ca}}$ and (c) $I_{K_{ur}}$. Columns are sensitivity coefficients for the (i) Colman–Zhang model (CZ) and (ii) Grandi–Bers model (GB) populations. Results for each AF subpopulation are plotted with open circles and those for the aggregate AF dataset are shown in bar plots. Complete set of sensitivity coefficients are illustrated in Figure S4. Given our definition of repolarization reserve, the parameter related to a given blocked current is associated with a large coefficient

and Grandi–Bers model populations (Figure S4), suggesting synergy in action potential duration prolongation when blocking the **rapid delayed rectifier K^+ current** (I_{K_r}) along with the atrial-predominant K^+ currents.

Values of coefficients for $G_{K_{2P}}$, $G_{K_{Ca}}$ and $G_{K_{ur}}$ are summarized in Table S5, allowing for quantitative comparison of interactions on ΔAPD . Note that the results of interactions in combined block were reciprocal, that is, similar results could be obtained by quantifying repolarization reserve via block of either current and computing the sensitivity of the other. Importantly, in both populations, these sensitivity coefficients were generally more positive at 3 Hz versus 1 Hz, indicating the synergistic action potential duration prolonging effects due to inhibition of multiple atrial-predominant K^+ -currents exhibit positive rate dependence.

3.5 | Interactions between effects of current inhibition confirmed in simulated multicurrent block

We verified the findings from sensitivity analysis of repolarization reserve by comparing the fractional ΔAPD following multicurrent block with the additive effects of individual current block. Specifically, interactions were deemed synergistic if the effect of combined current block was greater than the additive effects of individual current block or antagonistic with less-than-additive effect (Figure 6 and Figure S5). Combined $I_{K_{2P}} + I_{K_{Ca}}$ block consistently exhibited synergistic action potential duration prolongation in both Grandi–Bers and Colman–Zhang model populations. This was also seen in simulated combined block of $I_{K_{Ca}} + I_{K_{ur}}$ with Colman–Zhang model populations and most subpopulations with the Grandi–Bers model, consistent with the coefficients of $G_{K_{ur}}$ and $G_{K_{2P}}$ in Figure 5b. Interestingly, the pair $I_{K_{2P}} + I_{K_{ur}}$ exhibited competition in action potential duration prolongation at 1 Hz in the CZ model and this shifted towards synergy at 3 Hz, matching the predictions from the coefficients of $G_{K_{ur}}$ in Figure 5a, i. On the other hand, this pair ($I_{K_{2P}} + I_{K_{ur}}$) consistently displayed synergy at both pacing rates in Grandi–Bers model populations. Furthermore, combined block of all three atrial-predominant K^+ currents ($I_{K_{2P}} + I_{K_{Ca}} + I_{K_{ur}}$) exhibited stronger interactions, producing synergistic action potential duration prolongation for all Grandi–Bers model subpopulations and all Colman–Zhang model subpopulations at 3 Hz and many Colman–Zhang model subpopulations at 1 Hz. Importantly, in both model populations, synergy was stronger at 3 Hz versus 1 Hz. Note that these results match well with the sensitivity coefficients in Figure 5 and Table S5, in the sense that the extent and nature of the interactions agree well with the sign and magnitude of the sensitivity coefficients. The fact that the synergy was stronger at 3 Hz versus 1 Hz suggests that the synergistic action potential duration prolongation shows positive rate dependence, which is favourable for anti-AF pharmacotherapy.

We performed additional simulations with selected AF subpopulations (#1 and #5) to determine if the interactions persist when the currents were subjected to a broader range of blockade (Figure 7). Changing the extent of block generally did not alter the nature of synergism or antagonism, and the strength of the interaction exhibited positive “dose dependence”: competition (Figure 7a, $I_{K_{2P}} + I_{K_{ur}}$ and $I_{K_{2P}} + I_{K_{Ca}} + I_{K_{ur}}$ for subpopulation #1 at 1 Hz) or synergy (Figure 7, rest plots) were substantially enhanced when simulated current block was increased from 25% to 100%. Figure S6 depicts exemplary APs for $I_{K_{2P}} + I_{K_{ur}}$ block showing antagonism at 1 Hz but synergism at 3 Hz. Further, the interactions were generally stronger at 3 Hz versus 1 Hz, confirming positive rate dependence across all percentages of block.

3.6 | Multicurrent block interaction effects were also present in tissue

We evaluated changes in action potential duration, effective refractory period (ERP), conduction velocity (CV) and wavelength (WL) in

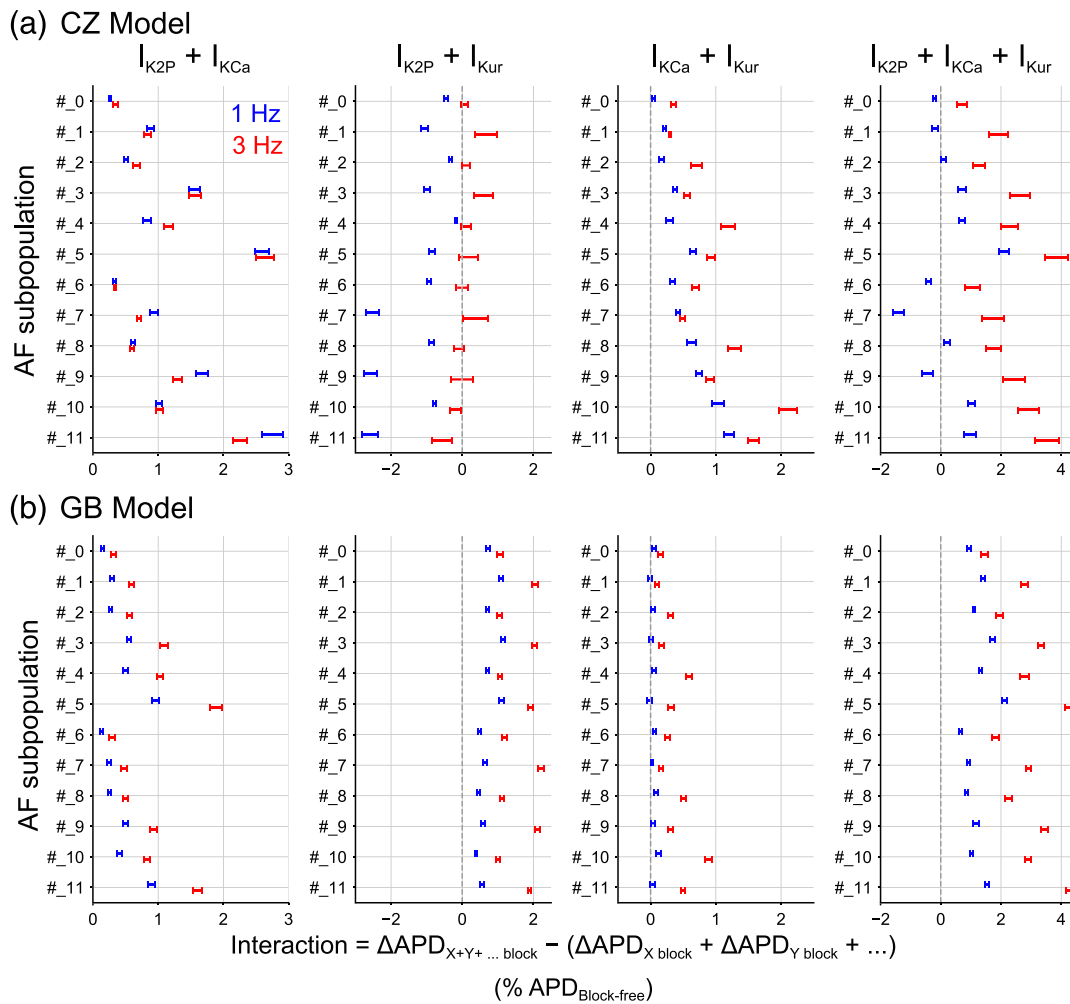


FIGURE 6 Interaction among I_{K2P} , I_{KCa} and I_{Kur} blockade in lengthening action potential duration. Confidence intervals were computed for the median interactions in multicurrent block defined as the difference in ΔAPD (action potential duration) for the combined effects versus the additive sum of separate effects. The interaction in ΔAPD is normalized to cell-matched block-free action potential duration. In these simulations, each current was subjected to 50% block. Positive interaction indicates synergism whereas negative difference suggests antagonism. Data of 1 Hz are shown in blue and 3 Hz in red

one dimensional tissues of two representative AF subpopulations (subpopulations #1 and #5) of the Colman-Zhang model population paced at both 1 and 3 Hz and considering both normal and reduced cell-to-cell electrical coupling in tissue (Figure 8, Figures S7–S10 and Table S6). Figure 8a illustrates an example of AP propagation in tissue and measurement of effective refractory period using the S1–S2 protocol. The modulating effects of atrial-predominant K^+ current block on action potential duration in tissue closely resembled those seen in the isolated cells (Figure 8b) and were also reflected in effective refractory period (Figure 8c). The effects of blocking these K^+ -currents on conduction velocity were negligible, although generally greater at 3 Hz versus 1 Hz (Figure S8 and Table S6). Consequently, the ΔWL due to K^+ -current block follows ΔAPD (Figure 8d). Indeed, positive rate dependence was generally observed for ΔAPD , ΔERP and ΔWL in groups involving I_{Kur} block (Figures S9 and S10).

Additionally, analysis of the confidence intervals for the median difference of ΔAPD , ΔERP and ΔWL between combined and individual current block (additive) effect in tissue confirmed the interactions

emerged at the cellular level (Figure S11). We found antagonism between I_{Kur} and I_{K2P} in lengthening action potential duration (APD), effective refractory period (ERP) and wavelength (WL) at 1 Hz and this shifted to synergy at 3 Hz. Further, the synergistic effects in tissue also generally exhibited positive rate dependence.

The results above in response to multi K^+ -channel block were maintained in the presence of reduced tissue coupling (Figures S7, S8B, S10, S11B and Table S6), to account for AF-induced gap junction remodelling and fibrosis (Burstein & Nattel, 2008), despite expected conduction velocity and wavelength reductions in the less-well coupled tissue (Table S6).

4 | DISCUSSION

Atrial-predominant and multichannel block are promising strategies for effective and safe antiarrhythmic pharmacotherapy in AF. We have evaluated effects of blocking multiple atrial-predominant K^+ currents (I_{Kur} , I_{K2P} , and I_{KCa}) on human atrial electrophysiologic

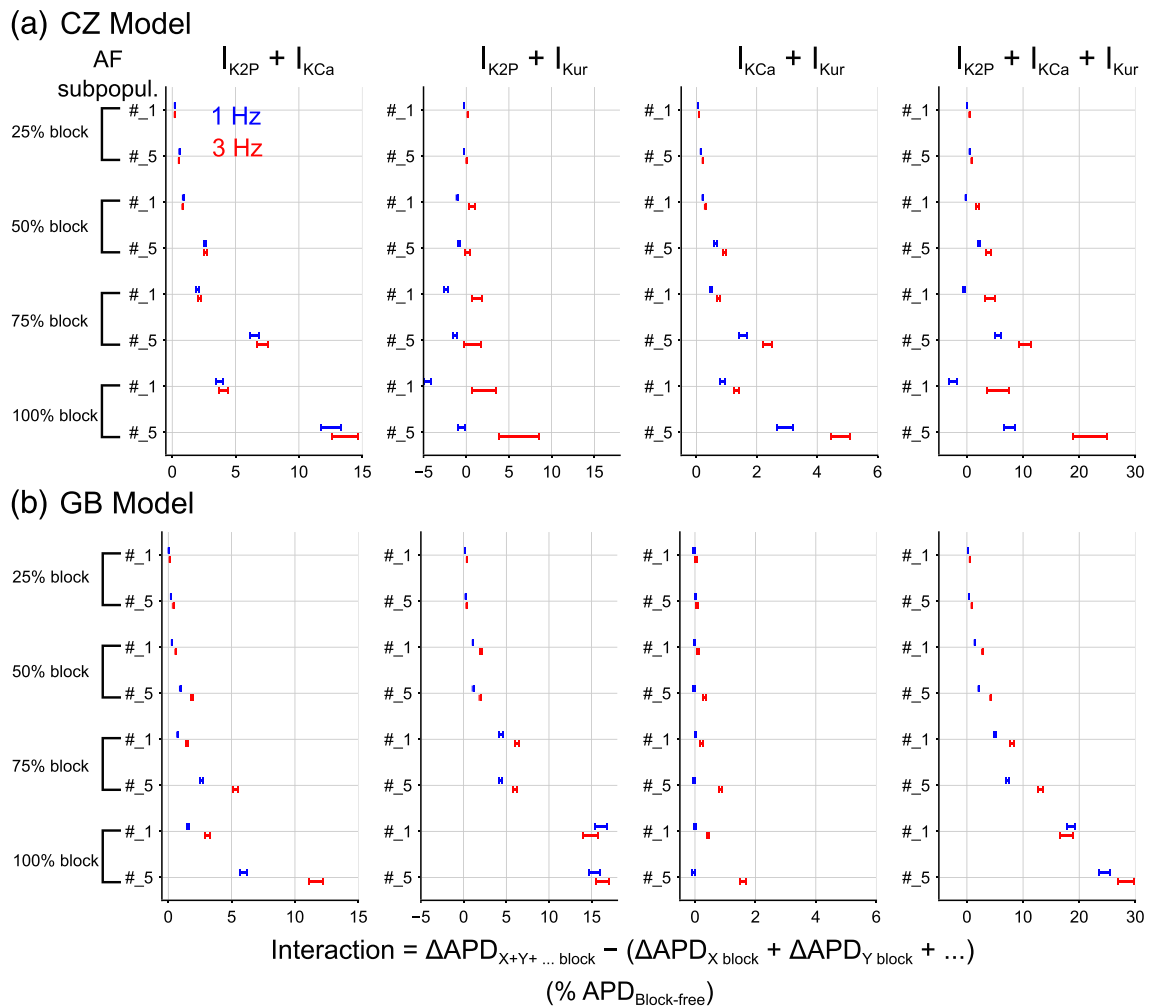


FIGURE 7 Dose dependence of interactions among multicurrent block on ΔAPD (action potential duration). Confidence intervals were computed for the median interactions in multicurrent block defined as the difference in ΔAPD for the combined effects versus the additive sum of separate effects for selected subpopulations when each current was subjected to 25% to 100% block. The interaction in ΔAPD is normalized to cell-matched block-free action potential duration. Positive difference indicates synergism whereas negative difference suggests antagonism. Data of 1 Hz are shown in blue and 3 Hz in red

parameters utilizing a population-based Quantitative Systems Pharmacology framework. Through sensitivity and statistical analyses of our atrial cell and tissue populations, we found that synergistic (i.e. greater than additive) action potential duration prolongation could be achieved by multi-atrial-predominant K^+ -current block and this synergy displayed favourable positive rate-dependence (Figure 6) and dose-dependence (Figure 7). Our study points to simultaneous block of two or more atrial-predominant currents as a valuable strategy for antiarrhythmic therapy in AF.

4.1 | Effects of atrial-predominant K^+ -current block

Inhibition of atrial-predominant currents, such as I_{Kur} , I_{K2P} , I_{KCa} and I_{KACh} , is a promising strategy for anti-AF pharmacological therapies to limit adverse proarrhythmic (ventricular) effects of antiarrhythmic drugs (Hancox et al., 2016; Ravens, 2017; Voigt & Dobrev, 2016).

However, atrial-predominant- K^+ current blockers have not yet been successful in producing significant antiarrhythmic effects in the clinic. For example, MK-0448, the first clinically studied I_{Kur} inhibitor, did not significantly prolong atrial refractoriness in healthy individuals (Pavri et al., 2012). A recent clinical trial, DIAGRAF-IKUR, was prematurely terminated as XEN-D0103 did not exert clinically relevant reduction in AF burden (Camm et al., 2019; Shunmugam et al., 2018). The efficacy of I_{KACh} blockers has been questioned, as [AZD2927](#) failed to prolong left atrial effective refractory period in atrial flutter patients (Walfridsson et al., 2015). Non-cardiac side effects have also drawn attention for blockers of I_{KACh} and I_{K2P} , whereas I_{KCa} modulators have yet to be tested in humans (Peyronnet & Ravens, 2019). In agreement with these clinical results, our simulation results demonstrated that 50% blockade of individual atrial-predominant K^+ current produced minor to moderate effects on action potential duration (Figures 3 and 4, Table S4), indicating moderate to low efficacy in suppressing AF circuits in the atria.

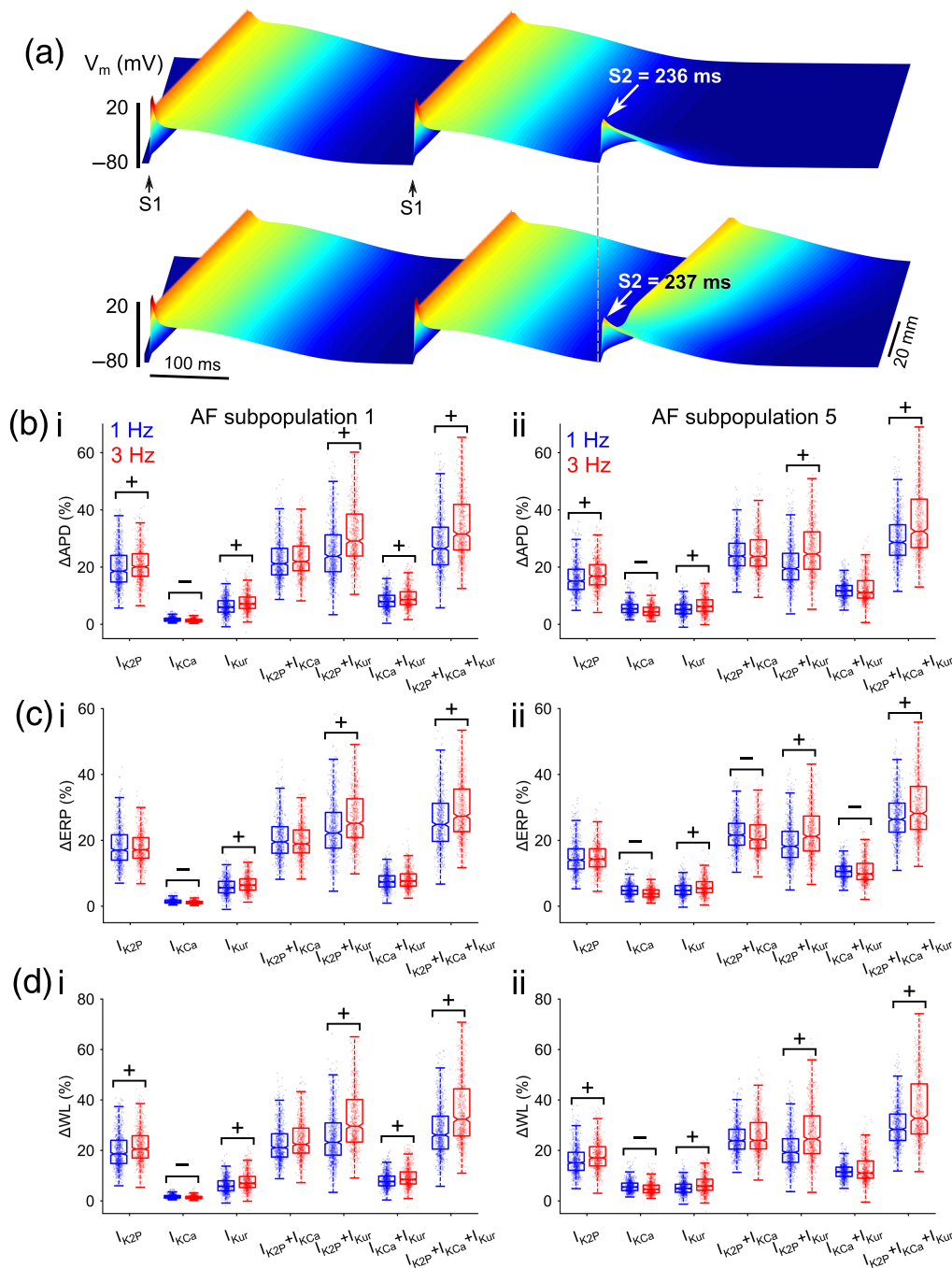


FIGURE 8 Effects of mono-K⁺ or multi-K⁺-current block on virtual atrial tissue populations using the Colman-Zhang model. (a) Example of AP propagation in one dimensional (1D) strand tissue paced at 3 Hz and measurement of effective refractory period (ERP) with an extra stimulus S₂, which failed at 236 ms (top row) but succeeded capturing tissue at 237 ms (bottom row). (b–d) Each row depicts change in (b) action potential duration (APD) (c) effective refractory period (ERP) and (d) wavelength (WL) due to current block obtained from virtual atrial strand populations paced at 1 Hz (blue) and 3 Hz (red). Each column describes results from (i) AF subpopulation 1 and (ii) AF subpopulation 5, respectively. WL was computed as the product of APD and conduction velocity (CV). Rate dependence (RD) deemed from analysis of CI in difference in 3 Hz versus 1 Hz in Figure S9, is shown as: “+” for positive RD and “-” for negative RD

4.2 | Synergistic antiarrhythmic effect of multiple atrial-predominant K⁺-current block

Multicurrent block has been increasingly recognized as an attractive strategy for AF management, based on the observation that most

clinically approved antiarrhythmic drugs target multiple ionic currents (Peyronnet & Ravens, 2019) and preclinical data demonstrating synergistic anti-AF effects of multicurrent block schemes (Aguilar et al., 2015; Kirchhoff et al., 2015, 2016; Ni et al., 2017; Reiffel et al., 2015). Application of multicurrent block regimens may therefore

have important implications, including increasing the efficacy of antiarrhythmic pharmacotherapy and reduction of unwanted adverse effects on the heart and non-cardiac systems through decreasing effective compound doses.

Here we combined the atrial-predominant and multicurrent block strategies as a novel anti-AF paradigm, and evaluated antiarrhythmic effects of simultaneously inhibiting multiple atrial-predominant K^+ currents on human atrial myocytes and tissues. To account for biological variability in atrial electrophysiology (including cell–cell and patient–patient variation, regional heterogeneity, and diverse aetiology and manifestation of AF), we employed two distinct human atrial models and simulated various degrees and combinations of AF-remodelling effects on I_{Kur} , I_{K2P} and I_{KCa} based on experimental data. The two models exhibited quantitative differences in action potential duration prolongation and rate-dependent changes (Figure 4). Yet, in both populations, combined block of these atrial-predominant currents substantially increased fractional action potential duration prolongation and enhanced its positive rate dependence as compared to block of each current individually. Our analyses revealed synergistic (greater than merely additive) action potential duration prolongation upon simulated multicurrent block (Figures 6), and this effect also increases with the degree of block (Figure 7). Importantly, this synergy in action potential duration prolongation consistently exhibited favourable positive rate dependence in the two distinct atrial model populations, despite some variability in the presence and strength of interaction within the AF subpopulations. Interestingly, in the Colman–Zhang model the pair $I_{K2P} + I_{Kur}$ displayed competition in lengthening action potential duration at 1 Hz; this interaction may limit excessive action potential duration prolongation at slow pacing rates thus preventing proarrhythmic (ectopy) events including early afterdepolarizations. Antiarrhythmic synergistic interactions also emerged in tissues, where myocytes were electrically coupled; simulated multicurrent block regimens produced interaction and rate dependence patterns consistent with single cell results for prolongation of in-tissue action potential duration, effective refractory period and, more importantly, wavelength, a biomarker frequently used to determine the required substrate size for re-entry circuit maintenance. Collectively, our results demonstrate that combined block of two or more atrial-predominant K^+ currents can exert synergistic and positive rate-dependent antiarrhythmic effects and therefore is a valuable therapeutic for AF.

Remarkably, additional atrial-ventricular differences can be employed to achieve atrial-selectivity for AF pharmacotherapy (Burashnikov, Diego, Zygmunt, Belardinelli, & Antzelevitch, 2007), including targeting of the atrial predominant I_{KACH} , which we have not incorporated as part of this initial investigation. Further, we (Ni et al., 2017) and others (Aguilar et al., 2015; Kirchhoff et al., 2015; Reiffel et al., 2015; Sicouri, Burashnikov, Belardinelli, & Antzelevitch, 2010) have previously shown that synergistic and atrial-selective antiarrhythmic effects can be achieved by combined block of Na^+ and K^+ currents. It remains to be tested whether combined Na^+ current and multiple atrial-predominant K^+ -current block displays favourable rate- and atrial-selective anti-AF effects.

4.3 | Sensitivity analysis for investigating rate dependence and interactions of multicurrent block

We successfully applied sensitivity analysis and statistical analysis of population-based model simulations to inform rate dependence and extended the approach to identify interactions between modulations of K^+ -current block on atrial action potential duration. To understand the influence of transmembrane current strength on action potential duration at both fast and slow pacing frequencies, we derived rate dependence coefficients B_{RD} as the difference in action potential duration sensitivity coefficients at the slow versus fast pacing rates (Figure 2) and validated that B_{RD} was a good predictor of rate dependence of action potential duration prolongation due to current blockade in subsequent simulations of K^+ -current block (Figure 4). Additionally, sensitivity analysis of repolarization reserve (quantified by ΔAPD following I_{Kr} block) has proven valuable to reveal the contribution of other ionic currents to ventricular repolarization reserve (Sarkar & Sobie, 2011). Here, we demonstrated that sensitivity analysis of repolarization reserve could also provide insight into the sign (synergy or competition) and extent of interactions of multicurrent blockade in lengthening action potential duration (Figure 5). The predicted interactions were confirmed through subsequent simulations of multicurrent block and comparisons to single-current block (Figures 6). These results suggest that sensitivity analysis of repolarization reserve is a powerful approach for dissecting interactive effects among block of multiple currents on modulating action potential duration. This method has broader applicability to other “atrial-selective” targets including I_{KACH} and the **fast Na^+ current**, I_{Na} (Ravens, Poulet, Wettwer, & Knaut, 2013), and systems models, for example, ventricular myocyte models.

4.4 | Model- and AP-shape independence of positive rate-dependent synergy of multicurrent block

It is well known that human atrial myocytes display at least three distinct characteristic AP morphologies; among them type-1 AP shows significant plateau phase 2 repolarization and type-3 AP exhibits triangular-shaped repolarization phases (Ravens et al., 2014; Wang et al., 1993; Workman et al., 2001). Hence, we ran simulations with two mathematical models of human atrial AP displaying distinct type-1 (Colman–Zhang model) and type-3 (Grandi–Bers model) AP morphologies. In fact, it is well appreciated that effects of I_{Kur} block on APD_{90} are dependent on baseline AP morphology (Wettwer et al., 2004; Workman et al., 2001), with both prolongation and shortening in APD_{90} being reported experimentally, and also seen in our previous modelling (Colman et al., 2017; Ellinwood et al., 2017a, 2017b). While some of the differences in model responses might be related to distinct AP morphologies, we cannot exclude model-dependencies due to distinct cellular model structure and models of ionic and Ca^{2+} handling processes. Interestingly, however, analyses using both models demonstrated that combined block of the three atrial-predominant K^+ currents enhanced positive rate dependence of

action potential duration prolongation and produced positively rate-dependent synergistic action potential duration prolongation. Collectively, these results demonstrate that combined blockade of the three currents consistently produced favourable anti-AF effects independent of the baseline electrophysiological characteristics and/or ionic remodelling effects.

Our biophysically detailed models allow investigating the mechanistic underpinnings of the favourable anti-AF consequences. For example, the mechanism underlying I_{Kur} (pore) block-mediated positive rate dependence was explained by the Nattel group with the increased relative contribution of I_{Kur} to AP repolarization at fast pacing rates due to reduced activation of I_{Kr} (Aguilar, Feng, Vigmond, Comtois, & Nattel, 2017). Nevertheless, the mechanisms underlying rate dependence of action potential duration change upon ion channel block are complex, and our preliminary analyses suggest that, in addition to the previously described mechanisms, rate-dependent changes in Na^+ and Ca^{2+} homeostasis mainly mediate the positive rate dependence of action potential duration, by both influencing the rate-dependent contribution of the atrial-predominant K^+ current (e.g. Ca^{2+} -dependent increase of I_{KCa}) and causing rate-dependent shifts in electrogenic Na^+ and Ca^{2+} transporters (Grandi et al., 2011). Future systematic investigations of these mechanisms are required.

4.5 | Limitations and future work

In this study, we simulated block of K^+ currents without describing any specific, existing compound or compound combinations, which are likely to exert off-target effects not considered here. We emphasize that we are not advocating reconsideration of previously failed drugs, but rather suggesting that in preclinical developments there are quantitative grounds for pursuing investigation of polytherapy targeting those atrial-predominant currents we have addressed here, which may also extend to other atrial-specific synergies.

While our approach shows promise, factors we have disregarded warrant discussion and should be addressed in future investigations. For example, other atrial-predominant targets could be included (e.g. I_{KACh} and I_{Na}), and the extent of blockade for each atrial-predominant K^+ current could be optimized to achieve desired antiarrhythmic effects while limiting drug doses. We have shown that synergy in prolonging action potential duration increases with the extent of current block, but our approach could be applied to simulating permutations of different degrees of channel block, to identify the optimal combination of targets and their relative block that maximize synergy. Additionally, while we simulated a simple pore block scheme, it might be important to incorporate state-dependence and use-dependence of channel blockers in evaluating realistic compounds (Ellinwood et al., 2017a, 2017b; Ni et al., 2017). State-dependent block models would require additional data describing the affinity of the drug compound to various channel conformational/gating modalities (e.g. open, closed, and/or inactivation state block), binding kinetics, drug polarity and charge for the drug-channel interaction (Yang et al., 2020). This type of information is relatively sparse for drugs

targeting the atrial predominant K^+ currents, particularly relative to the binding characteristics of Na^+ channel blockers, which are much better characterized and known to play an important role for atrial selective I_{Na} block (Burashnikov et al., 2007; Morotti et al., 2016). Specific data are available that characterize binding mechanisms for I_{Kur} (Lagrutta, Wang, Fermini, & Salata, 2006) and differing modes of block (pore-block versus modulatory) and their regulation by voltage and pH are known differentiating characteristics for I_{KCa} inhibitors (Brown, Shim, Christophersen, & Wulff, 2020). Less extensive characterization is available for I_{K2P} antagonists, although many AF-relevant drugs are known to inhibit the **TASK-1** channels simulated here. The range of questions evoked by including model variations for these characteristics would be poorly constrained at this point and applying modelling approaches to explore the possible alterations due to those dynamic effects is far beyond the scope of the current study. However, questions of that type provide an excellent basis for extending understanding of the synergistic characteristics we have observed here. Further, while we can simply simulate certain degrees of current block, the cellular concentrations of a same systemic drug dose can vary across individuals. Thus, future studies should account for both (population) pharmacokinetic (PK) and pharmacodynamic (PD) drug interactions.

Although both the Colman-Zhang and Grandi-Bers models have been well established and widely used, it is worth noting that the APD_{90} produced from the two models are lower than those from the experimental measurements (Figure 1). This limitation might be explained by the fact that the models were originally built to reflect different experimental sources and that published human atrial myocyte data are quite variable and is mitigated, at least in part, by the use of two model populations that account for some of the variability.

We calibrated our model populations to the observed experimental ranges. Calibration to experimental distribution (Lawson et al., 2018) could be implemented in future studies to attain model populations with higher fidelity of clinical variabilities. Although we started from well-validated baseline models, since we only used action potential duration and resting membrane potential as biomarkers, parameter unidentifiability is a potential limitation, which could be attenuated if broader experimental datasets were available. Further, we simulated AF model populations with variable degrees of AF-remodelling. As AF is a progressive disease, the proposed multiple atrial-predominant-current block might have different efficacy for various AF stages, e.g. in paroxysmal AF, which displays distinct AP and Ca^{2+} biomarkers compared to chronic AF (Nattel & Dobrev, 2016). The complexity of AF-related fibrosis (Burstein & Nattel, 2008) may present complex tissue responses to the proposed multicurrent block strategy and require more realistic heterogenous descriptions in tissue simulations (Zahid et al., 2016).

We analysed the effects of current block by quantifying changes in APD_{90} at the cellular level and effective refractory period and wavelength in tissue. This approach is consistent with the accepted mechanisms of action of class III antiarrhythmics, but is limited in that it required exclusion of model variants exhibiting action potential

duration alternans, which prevented Δ APD analysis. Nevertheless, mechanisms underlying both AF and antiarrhythmic drugs' action are highly complex and future investigations might account for composite metrics (Yang et al., 2016), including, for example APD₅₀, Ca²⁺-related biomarkers (Ellinwood et al., 2017a, 2017b), presence of afterdepolarizations or alternans, and AP propagation dynamics in tissue.

Autonomic regulation of atrial function contributes importantly to the onset and maintenance of AF (Linz et al., 2019). The autonomic nervous system regulates atrial electrophysiology and modulates the function of multiple atrial-predominant currents, for example I_{K,ACh}, which becomes constitutively active in AF (Dobrev et al., 2005). Therefore, it may be important to incorporate autonomic regulations in future pharmacology investigations.

4.6 | Conclusions

Using state-of-the-art Quantitative Systems Pharmacology approaches, we showed that multi-atrial-predominant K⁺-current block produces favourable positive rate-dependent synergistic antiarrhythmic effects, suggesting that this strategy may be effective against AF and limit cardiac side effects.

ACKNOWLEDGEMENTS

We would like to thank the Clinical and Translational Science Center and Dr. Matteo Farnè at the Department of Statistics, University of California, Davis, for advice on statistical analyses. This work was supported by the American Heart Association Postdoctoral Fellowship 20POST35120462 (H.N.) and Grant 15SDG24910015 (E.G.), the UC Davis School of Medicine Dean's Fellow Award (E.G.); the National Institutes of Health (NIH) Stimulating Peripheral Activity to Relieve Conditions Grant 1OT2OD026580-01 (E.G.); the National Heart, Lung, and Blood Institute Grants R01HL131517, R01HL141214, and P01HL141084 (E.G.) and K99HL138160 (S.M.); the Health and Environmental Sciences Institute Grant U01FD006676-01 (A.E.).

AUTHOR CONTRIBUTIONS

H.N. and E.G. designed the research. H.N. performed the research. H.N., A.F.I., W.R.G., S.M.N., H.Z., A.G.E., S.M., and E.G. analysed the data. H.N. and E.G. wrote the manuscript. A.F.I., W.R.G., S.M.N., H.Z., A.G.E., and S.M. revised the manuscript.

CONFLICT OF INTEREST

The authors declare no conflict of interest.

DECLARATION OF TRANSPARENCY AND SCIENTIFIC RIGOUR

This Declaration acknowledges that this paper adheres to the principles for transparent reporting and scientific rigour of preclinical research as stated in the *BJP* guidelines for [Design and Analysis](#) and as recommended by funding agencies, publishers and other organisations engaged with supporting research.

ORCID

Haibo Ni  <https://orcid.org/0000-0003-0083-4286>

Eleonora Grandi  <https://orcid.org/0000-0002-4401-8857>

REFERENCES

- Aguilar, M., Feng, J., Vigmond, E., Comtois, P., & Nattel, S. (2017). Rate-dependent role of IK_r in human atrial repolarization and atrial fibrillation maintenance. *Biophysical Journal*, 112, 1997–2010. <https://doi.org/10.1016/j.bpj.2017.03.022>
- Aguilar, M., Xiong, F., Qi, X. Y., Comtois, P., & Nattel, S. (2015). Potassium channel blockade enhances atrial fibrillation-selective antiarrhythmic effects of optimized state-dependent sodium channel blockade. *Circulation*, 132, 2203–2211. <https://doi.org/10.1161/CIRCULATIONAHA.115.018016>
- Alexander, S. P., Mathie, A., Peters, J. A., Veale, E. L., Striessnig, J., Kelly, E., ... Sharman, J. L. (2019). The concise guide to pharmacology 2019/20: Ion channels. *British Journal of Pharmacology*, 176, S142–S228.
- Bers, D. M., & Grandi, E. (2011). Human atrial fibrillation: Insights from computational electrophysiological models. *Trends in Cardiovascular Medicine*, 21, 145–150. <https://doi.org/10.1016/j.tcm.2012.04.004>
- Bosch, R. F., Zeng, X., Grammer, J. B., Popovic, K., Mewis, C., & Kühlkamp, V. (1999). Ionic mechanisms of electrical remodeling in human atrial fibrillation. *Cardiovascular Research*, 44, 121–131. [https://doi.org/10.1016/S0008-6363\(99\)00178-9](https://doi.org/10.1016/S0008-6363(99)00178-9)
- Britton, O. J., Bueno-Orovio, A., Ammel, K. V., Lu, H. R., Towart, R., Gallacher, D. J., & Rodriguez, B. (2013). Experimentally calibrated population of models predicts and explains intersubject variability in cardiac cellular electrophysiology. *Proceedings of the National Academy of Sciences*, 110, E2098–E2105. <https://doi.org/10.1073/pnas.1304382110>
- Brown, B. M., Shim, H., Christophersen, P., & Wulff, H. (2020). Pharmacology of small- and intermediate-conductance calcium-activated potassium channels. *Annual Review of Pharmacology and Toxicology*, 60, 219–240. <https://doi.org/10.1146/annurev-pharmtox-010919-023420>
- Burashnikov, A., Diego, J. M. D., Zygmunt, A. C., Belardinelli, L., & Antzelevitch, C. (2007). Atrium-selective sodium channel block as a strategy for suppression of atrial fibrillation differences in sodium channel inactivation between atria and ventricles and the role of ranolazine. *Circulation*, 116, 1449–1457. <https://doi.org/10.1161/CIRCULATIONAHA.107.704890>
- Burstein, B., & Nattel, S. (2008). Atrial fibrosis: Mechanisms and clinical relevance in atrial fibrillation. *Journal of the American College of Cardiology*, 51, 802–809. <https://doi.org/10.1016/j.jacc.2007.09.064>
- Caballero, R., de la Fuente, M. G., Gómez, R., Barana, A., Amorós, I., Dolz-Gaitón, P., ... Delpón, E. (2010). In humans, chronic atrial fibrillation decreases the transient outward current and ultrarapid component of the delayed rectifier current differentially on each atria and increases the slow component of the delayed rectifier current in both. *Journal of the American College of Cardiology*, 55, 2346–2354. <https://doi.org/10.1016/j.jacc.2010.02.028>
- Calvo, D., Filgueiras-Rama, D., & Jalife, J. (2018). Mechanisms and drug development in atrial fibrillation. *Pharmacological Reviews*, 70, 505–525. <https://doi.org/10.1124/pr.117.014183>
- Camm, A. J., Dorian, P., Hohnloser, S. H., Kowey, P. R., Tyl, B., Ni, Y., ... Sanders, P. (2019). A randomized, double-blind, placebo-controlled trial assessing the efficacy of S66913 in patients with paroxysmal atrial fibrillation. *European Heart Journal—Cardiovascular Pharmacotherapy*, 5, 21–28. <https://doi.org/10.1093/ehjcvp/pyy022>
- Colman, M. A., Aslanidi, O. V., Kharache, S., Boyett, M. R., Garratt, C., Hancox, J. C., & Zhang, H. (2013). Pro-arrhythmogenic effects of atrial fibrillation-induced electrical remodeling: insights from the three-dimensional virtual human atria. *The Journal of Physiology*, 591, 4249–4272. <https://doi.org/10.1113/jphysiol.2013.254987>

- Colman, M. A., Ni, H., Liang, B., Schmitt, N., & Zhang, H. (2017). In silico assessment of genetic variation in KCNA5 reveals multiple mechanisms of human atrial arrhythmogenesis. *PLoS Computational Biology*, *13*, e1005587. <https://doi.org/10.1371/journal.pcbi.1005587>
- Cummins, M. A., Dalal, P. J., Bugana, M., Severi, S., & Sobie, E. A. (2014). Comprehensive analyses of ventricular myocyte models identify targets exhibiting favorable rate dependence. *PLoS Computational Biology*, *10*, e1003543. <https://doi.org/10.1371/journal.pcbi.1003543>
- Curtis, M. J., Alexander, S., Cirino, G., Docherty, J. R., George, C. H., Giembycz, M. A., ... Ahluwalia, A. (2018). Experimental design and analysis and their reporting II: Updated and simplified guidance for authors and peer reviewers. *British Journal of Pharmacology*, *175*, 987–993. <https://doi.org/10.1111/bph.14153>
- Dobrev, D., Friedrich, A., Voigt, N., Jost, N., Wettwer, E., Christ, T., ... Ravens, U. (2005). The G protein-gated potassium Current IK_{ACH}s constitutively active in patients with chronic atrial fibrillation. *Circulation*, *112*, 3697–3706. <https://doi.org/10.1161/CIRCULATIONAHA.105.575332>
- Ellinwood, N., Dobrev, D., Morotti, S., & Grandi, E. (2017a). In silico assessment of efficacy and safety of IK_{ur} inhibitors in chronic atrial fibrillation: Role of kinetics and state-dependence of drug binding. *Frontiers in Pharmacology*, *8*, 799. <https://doi.org/10.3389/fphar.2017.00799>
- Ellinwood, N., Dobrev, D., Morotti, S., & Grandi, E. (2017b). Revealing kinetics and state-dependent binding properties of IK_{ur}-targeting drugs that maximize atrial fibrillation selectivity. *Chaos: An Interdisciplinary Journal of Nonlinear Science*, *27*, 093918. <https://doi.org/10.1063/1.5000226>
- Ford, J., Milnes, J., El Haou, S., Wettwer, E., Loose, S., Matschke, K., ... Ravens, U. (2016). The positive frequency-dependent electrophysiological effects of the IK_{ur} inhibitor XEN-DO103 are desirable for the treatment of atrial fibrillation. *Heart Rhythm*, *13*, 555–564. <https://doi.org/10.1016/j.hrthm.2015.10.003>
- Gonzalez de la Fuente, M., Barana, A., Gomez, R., Amoros, I., Dolz-Gaiton, P., Sacristan, S., ... Caballero, R. (2012). Chronic atrial fibrillation up-regulates 1-adrenoceptors affecting repolarizing currents and action potential duration. *Cardiovascular Research*, *97*, 379–388.
- Grammer, J. B., Bosch, R. F., Kühlkamp, V., & Seipel, L. (2000). Molecular remodeling of Kv4.3 potassium channels in human atrial fibrillation. *Journal of Cardiovascular Electrophysiology*, *11*, 626–633. <https://doi.org/10.1111/j.1540-8167.2000.tb00024.x>
- Grandi, E., Dobrev, D., & Heijman, J. (2019). Computational modeling: What does it tell us about atrial fibrillation therapy? *International Journal of Cardiology*, *287*, 155–161. <https://doi.org/10.1016/j.ijcard.2019.01.077>
- Grandi, E., & Maleckar, M. M. (2016). Anti-arrhythmic strategies for atrial fibrillation: The role of computational modeling in discovery, development, and optimization. *Pharmacology & Therapeutics*, *168*, 126–142. <https://doi.org/10.1016/j.pharmthera.2016.09.012>
- Grandi, E., Pandit, S. V., Voigt, N., Workman, A. J., Dobrev, D., Jalife, J., & Bers, D. M. (2011). Human atrial action potential and Ca²⁺ model sinus rhythm and chronic atrial fibrillation. *Circulation Research*, *109*, 1055–1066. <https://doi.org/10.1161/CIRCRESAHA.111.253955>
- Hancox, J. C., James, A. F., Marrion, N. V., Zhang, H., & Thomas, D. (2016). Novel ion channel targets in atrial fibrillation. *Expert Opinion on Therapeutic Targets*, *20*, 947–958. <https://doi.org/10.1517/14728222.2016.1159300>
- Hansson, A., Holm, M., Blomström, P., Johansson, R., Lührs, C., Brandt, J., & Olsson, S. B. (1998). Right atrial free wall conduction velocity and degree of anisotropy in patients with stable sinus rhythm studied during open heart surgery. *European Heart Journal*, *19*, 293–300. <https://doi.org/10.1053/euhj.1997.0742>
- Harding, S. D., Sharman, J. L., Faccenda, E., Southan, C., Pawson, A. J., Ireland, S., ... NC-IUPHAR. (2018). The IUPHAR/BPS guide to pharmacology in 2018: Updates and expansion to encompass the new guide to Immunopharmacology. *Nucleic Acids Research*, *46*, D1091–D1106. <https://doi.org/10.1093/nar/gkx1121>
- Kirchhoff, J. E., Diness, J. G., Abildgaard, L., Sheykhzade, M., Grunnet, M., & Jespersen, T. (2016). Antiarrhythmic effect of the Ca²⁺-activated K⁺ (SK) channel inhibitor ICA combined with either amiodarone or dofetilide in an isolated heart model of atrial fibrillation. *Pflügers Archiv - European Journal of Physiology*, *468*, 1853–1863. <https://doi.org/10.1007/s00424-016-1883-9>
- Kirchhoff, J. E., Goldin Diness, J., Sheykhzade, M., Grunnet, M., & Jespersen, T. (2015). Synergistic antiarrhythmic effect of combining inhibition of Ca²⁺-activated K⁺ (SK) channels and voltage-gated Na⁺ channels in an isolated heart model of atrial fibrillation. *Heart Rhythm*, *12*, 409–418. <https://doi.org/10.1016/j.hrthm.2014.12.010>
- Krul, S. P. J., Berger, W. R., Smit, N. W., van Amersfoorth, S. C. M., Driessen, A. H. G., van Boven, W. J., ... de Groot, J. R. (2015). Atrial fibrosis and conduction slowing in the left atrial appendage of patients undergoing thoracoscopic surgical pulmonary vein isolation for atrial fibrillation. *Circulation. Arrhythmia and Electrophysiology*, *8*, 288–295. <https://doi.org/10.1161/CIRCEP.114.001752>
- Lagrutta, A., Wang, J., Fermini, B., & Salata, J. J. (2006). Novel, potent inhibitors of human Kv1.5 K⁺ channels and ultrarapidly activating delayed rectifier potassium current. *The Journal of Pharmacology and Experimental Therapeutics*, *317*, 1054–1063. <https://doi.org/10.1124/jpet.106.101162>
- Lawson, B. A. J., Drovandi, C. C., Cusimano, N., Burrage, P., Rodriguez, B., & Burrage, K. (2018). Unlocking data sets by calibrating populations of models to data density: A study in atrial electrophysiology. *Science Advances*, *4*, e1701676. <https://doi.org/10.1126/sciadv.1701676>
- Linz, D., Elliott, A. D., Hohl, M., Malik, V., Schotten, U., Dobrev, D., ... Sanders, P. (2019). Role of autonomic nervous system in atrial fibrillation. *International Journal of Cardiology*, *287*, 181–188. <https://doi.org/10.1016/j.ijcard.2018.11.091>
- Morotti, S., & Grandi, E. (2017). Logistic regression analysis of populations of electrophysiological models to assess proarrhythmic risk. *MethodsX*, *4*, 25–34. <https://doi.org/10.1016/j.mex.2016.12.002>
- Morotti, S., McCulloch, A. D., Bers, D. M., Edwards, A. G., & Grandi, E. (2016). Atrial-selective targeting of arrhythmogenic phase-3 early afterdepolarizations in human myocytes. *Journal of Molecular and Cellular Cardiology*, *96*, 63–71. <https://doi.org/10.1016/j.yjmcc.2015.07.030>
- Muskiewicz, A., Britton, O. J., Gemmell, P., Passini, E., Sánchez, C., Zhou, X., ... Rodriguez, B. (2016). Variability in cardiac electrophysiology: Using experimentally-calibrated populations of models to move beyond the single virtual physiological human paradigm. *Progress in Biophysics and Molecular Biology*, *120*, 115–127. <https://doi.org/10.1016/j.pbiomolbio.2015.12.002>
- Narayan, S. M., Franz, M. R., Clopton, P., Pruvot, E. J., & Krummen, D. E. (2011). Repolarization alternans reveals vulnerability to human atrial fibrillation. *Circulation*, *123*, 2922–2930. <https://doi.org/10.1161/CIRCULATIONAHA.110.977827>
- Nattel, S., & Dobrev, D. (2016). Electrophysiological and molecular mechanisms of paroxysmal atrial fibrillation. *Nature Reviews. Cardiology*, *13*, 575–590. <https://doi.org/10.1038/nrcardio.2016.118>
- Ni, H., Morotti, S., & Grandi, E. (2018). A heart for diversity: Simulating variability in cardiac arrhythmia research. *Frontiers in Physiology*, *9*, 958. <https://doi.org/10.3389/fphys.2018.00958>
- Ni, H., Whittaker, D. G., Wang, W., Giles, W. R., Narayan, S. M., & Zhang, H. (2017). Synergistic anti-arrhythmic effects in human atria with combined use of sodium blockers and acacetin. *Frontiers in Physiology*, *8*, 946. <https://doi.org/10.3389/fphys.2017.00946>
- Ni, H., Zhang, H., Grandi, E., Narayan, S. M., & Giles, W. R. (2019). Transient outward K⁺ current can strongly modulate action potential duration and initiate alternans in the human atrium. *American Journal of*

- Physiology. Heart and Circulatory Physiology*, 316, H527–H542. <https://doi.org/10.1152/ajpheart.00251.2018>
- Ozgen, N., Dun, W., Sosunov, E., Anyukhovskiy, E., Hirose, M., Duffy, H., ... Rosen, M. R. (2007). Early electrical remodeling in rabbit pulmonary vein results from trafficking of intracellular SK2 channels to membrane sites. *Cardiovascular Research*, 75, 758–769. <https://doi.org/10.1016/j.cardiores.2007.05.008>
- Passini, E., Britton, O. J., Lu, H. R., Rohrbacher, J., Hermans, A. N., Gallacher, D. J., ... Rodriguez, B. (2017). Human in silico drug trials demonstrate higher accuracy than animal models in predicting clinical pro-arrhythmic cardiotoxicity. *Frontiers in Physiology*, 8. <https://doi.org/10.3389/fphys.2017.00668>
- Pavri, B. B., Greenberg, H. E., Kraft, W. K., Lazarus, N., Lynch, J. J., Salata, J. J., ... Bloomfield, D. (2012). Mk-0448, a specific Kv1.5 inhibitor safety, pharmacokinetics, and pharmacodynamic electrophysiology in experimental animal models and humans. *Circulation. Arrhythmia and Electrophysiology*, 5, 1193–1201. <https://doi.org/10.1161/CIRCEP.111.969782>
- Peyronnet, R., Ravens, U. (2019). Atria-selective antiarrhythmic drugs in need of alliance partners. *Pharmacological Research*, 145, 104262. <https://doi.org/10.1016/j.phrs.2019.104262>
- Qi, X.-Y., Diness, J. G., Brundel, B. J. J. M., Zhou, X.-B., Naud, P., Wu, C.-T., ... Nattel, S. (2014). Role of small-conductance calcium-activated potassium channels in atrial electrophysiology and fibrillation in the dog. *Circulation*, 129, 430–440. <https://doi.org/10.1161/CIRCULATIONAHA.113.003019>
- Ravens, U. (2017). Atrial-selective K⁺ channel blockers: Potential antiarrhythmic drugs in atrial fibrillation? *Canadian Journal of Physiology and Pharmacology*, 95, 1313–1318. <https://doi.org/10.1139/cjpp-2017-0024>
- Ravens, U., Katircioglu-Öztürk, D., Wettwer, E., Christ, T., Dobrev, D., Voigt, N., ... Matschke, K. (2014). Application of the RIMARC algorithm to a large data set of action potentials and clinical parameters for risk prediction of atrial fibrillation. *Medical & Biological Engineering & Computing*, 53, 263–273.
- Ravens, U., Poulet, C., Wettwer, E., & Knaut, M. (2013). Atrial selectivity of antiarrhythmic drugs. *The Journal of Physiology*, 591, 4087–4097. <https://doi.org/10.1113/jphysiol.2013.256115>
- Reiffel, J. A., Camm, A. J., Belardinelli, L., Zeng, D., Karwatowska-Prokopczuk, E., Olmsted, A., ... HARMONY Investigators. (2015). The HARMONY trial: Combined ranolazine and dronedarone in the management of paroxysmal atrial fibrillation: Mechanistic and therapeutic synergism. *Circulation. Arrhythmia and Electrophysiology*, 8, 1048–1056. <https://doi.org/10.1161/CIRCEP.115.002856>
- Sarkar, A. X., & Sobie, E. A. (2011). Quantification of repolarization reserve to understand inter-patient variability in the response to proarrhythmic drugs: A computational analysis. *Heart Rhythm: The Official Journal of the Heart Rhythm Society*, 8, 1749–1755. <https://doi.org/10.1016/j.hrthm.2011.05.023>
- Schmidt, C., Wiedmann, F., Voigt, N., Zhou, X.-B., Heijman, J., Lang, S., ... Thomas, D. (2015). Upregulation of K2P3.1 K⁺ current causes action potential shortening in patients with chronic atrial fibrillation. *Circulation*, 132, 82–92. <https://doi.org/10.1161/CIRCULATIONAHA.114.012657>
- Schmidt, C., Wiedmann, F., Zhou, X.-B., Heijman, J., Voigt, N., Ratte, A., ... De Simone, R. (2017). Inverse remodelling of K2P3.1 K⁺ channel expression and action potential duration in left ventricular dysfunction and atrial fibrillation: Implications for patient-specific antiarrhythmic drug therapy. *European Heart Journal*, 38, 1764–1774.
- Shunmugam, S. R., Sugihara, C., Freemantle, N., Round, P., Furniss, S., & Sulke, N. (2018). A double-blind, randomised, placebo-controlled, cross-over study assessing the use of XEN-D0103 in patients with paroxysmal atrial fibrillation and implanted pacemakers allowing continuous beat-to-beat monitoring of drug efficacy. *Journal of Interventional Cardiac Electrophysiology*, 51, 191–197.
- Sicouri, S., Burashnikov, A., Belardinelli, L., & Antzelevitch, C. (2010). Synergistic electrophysiologic and antiarrhythmic effects of the combination of ranolazine and chronic amiodarone in canine atria. *Circulation. Arrhythmia and Electrophysiology*, 3, 88–95. <https://doi.org/10.1161/CIRCEP.109.886275>
- Skibsbjerg, L., Jespersen, T., Christ, T., Maleckar, M. M., van den Brink, J., Tavi, P., & Koivumäki, J. T. (2016). Refractoriness in human atria: Time and voltage dependence of sodium channel availability. *Journal of Molecular and Cellular Cardiology*, 101, 26–34. <https://doi.org/10.1016/j.yjmcc.2016.10.009>
- Skibsbjerg, L., Poulet, C., Diness, J. G., Bentzen, B. H., Yuan, L., Kappert, U., ... Jespersen, T. (2014). Small-conductance calcium-activated potassium (SK) channels contribute to action potential repolarization in human atria. *Cardiovascular Research*, 103, 156–167. <https://doi.org/10.1093/cvr/cvu121>
- So, P. P.-S., Hu, X.-D., Backx, P. H., Puglisi, J. L., & Dorian, P. (2006). Blockade of IKs by HMR 1556 increases the reverse rate-dependence of refractoriness prolongation by dofetilide in isolated rabbit ventricles. *British Journal of Pharmacology*, 148, 255–263. <https://doi.org/10.1038/sj.bjp.0706721>
- Sobie, E. A. (2009). Parameter sensitivity analysis in electrophysiological models using multivariable regression. *Biophysical Journal*, 96, 1264–1274. <https://doi.org/10.1016/j.bpj.2008.10.056>
- Varró, A., & Baczkó, I. (2011). Cardiac ventricular repolarization reserve: A principle for understanding drug-related proarrhythmic risk. *British Journal of Pharmacology*, 164, 14–36. <https://doi.org/10.1111/j.1476-5381.2011.01367.x>
- Virág, L., Acsai, K., Hála, O., Zaza, A., Bitay, M., Bogáts, G., ... Varró, A. (2009). Self-augmentation of the lengthening of repolarization is related to the shape of the cardiac action potential: implications for reverse rate dependency. *British Journal of Pharmacology*, 156, 1076–1084. <https://doi.org/10.1111/j.1476-5381.2009.00116.x>
- Voigt, N., & Dobrev, D. (2016). Atrial-selective potassium channel blockers. *Cardiac Electrophysiology Clinics*, 8, 411–421. <https://doi.org/10.1016/j.ccep.2016.02.005>
- Wagoner, D. R. V., Pond, A. L., McCarthy, P. M., Trimmer, J. S., & Nerbonne, J. M. (1997). Outward K⁺ current densities and Kv1.5 expression are reduced in chronic human atrial fibrillation. *Circulation Research*, 80, 772–781. <https://doi.org/10.1161/01.RES.80.6.772>
- Walfridsson, H., Anfinsen, O.-G., Berggren, A., Frison, L., Jensen, S., Linhardt, G., ... Carlsson, L. (2015). Is the acetylcholine-regulated inwardly rectifying potassium current a viable antiarrhythmic target? Translational discrepancies of AZD2927 and A7071 in dogs and humans. *Europace: European Pacing, Arrhythmias, and Cardiac Electrophysiology: Journal of the Working Groups on Cardiac Pacing, Arrhythmias, and Cardiac Cellular Electrophysiology of the European Society of Cardiology*, 17, 473–482.
- Wang, Z., Fermini, B., & Nattel, S. (1993). Delayed rectifier outward current and repolarization in human atrial myocytes. *Circulation Research*, 73, 276–285. <https://doi.org/10.1161/01.RES.73.2.276>
- Wang, Z. G., Pelletier, L. C., Talajic, M., & Nattel, S. (1990). Effects of flecainide and quinidine on human atrial action potentials. Role of rate-dependence and comparison with guinea pig, rabbit, and dog tissues. *Circulation*, 82, 274–283. <https://doi.org/10.1161/01.CIR.82.1.274>
- Wettwer, E., Hála, O., Christ, T., Heubach, J. F., Dobrev, D., Knaut, M., ... Ravens, U. (2004). Role of IK_{ur} in controlling action potential shape and contractility in the human atrium influence of chronic atrial fibrillation. *Circulation*, 110, 2299–2306. <https://doi.org/10.1161/01.CIR.0000145155.60288.71>
- Workman, A. J., Kane, K. A., & Rankin, A. C. (2001). The contribution of ionic currents to changes in refractoriness of human atrial myocytes associated with chronic atrial fibrillation. *Cardiovascular Research*, 52, 226–235. [https://doi.org/10.1016/S0008-6363\(01\)00380-7](https://doi.org/10.1016/S0008-6363(01)00380-7)

- Yang, P.-C., DeMarco, K. R., Aghasafari, P., Jeng, M.-T., Dawson, J. R. D., Bekker, S., ... Clancy, C. E. (2020). A computational pipeline to predict cardiotoxicity: From the atom to the rhythm. *Circulation Research*, *126*, 947–964. <https://doi.org/10.1161/CIRCRESAHA.119.316404>
- Yang, P.-C., El-Bizri, N., Romero, L., Giles, W. R., Rajamani, S., Belardinelli, L., & Clancy, C. E. (2016). A computational model predicts adjunctive pharmacotherapy for cardiac safety via selective inhibition of the late cardiac Na current. *Journal of Molecular and Cellular Cardiology*, *99*, 151–161. <https://doi.org/10.1016/j.yjmcc.2016.08.011>
- Yap, Y. G., & Camm, A. J. (2003). Drug induced QT prolongation and torsades de pointes. *Heart*, *89*, 1363–1372. <https://doi.org/10.1136/heart.89.11.1363>
- Yuan, Y., Bai, X., Luo, C., Wang, K., & Zhang, H. (2015). The virtual heart as a platform for screening drug cardiotoxicity. *British Journal of Pharmacology*, *172*, 5531–5547. <https://doi.org/10.1111/bph.12996>
- Zahid, S., Cochet, H., Boyle, P. M., Schwarz, E. L., Whyte, K. N., Vigmond, E. J., ... Trayanova, N. A. (2016). Patient-derived models link

re-entrant driver localization in atrial fibrillation to fibrosis spatial pattern. *Cardiovascular Research*, *110*, 443–454. <https://doi.org/10.1093/cvr/cvw073>

SUPPORTING INFORMATION

Additional supporting information may be found online in the Supporting Information section at the end of this article.

How to cite this article: Ni H, Fogli Iseppa A, Giles WR, et al.

Populations of in silico myocytes and tissues reveal synergy of multiatrial-predominant K^+ -current block in atrial fibrillation.

Br J Pharmacol. 2020;177:4497–4515. <https://doi.org/10.1111/bph.15198>